

REVIEW ARTICLE

Metal-insulator transition in two-dimensional electron systems

S V Kravchenko

Physics Department, Northeastern University, Boston, MA 02115, USA

M P Sarachik

Physics Department, City College of the City University of New York, New York, NY 10031, USA

Abstract. The interplay between strong Coulomb interactions and randomness has been a long-standing problem in condensed matter physics. According to the scaling theory of localization, in two-dimensional systems of noninteracting or weakly interacting electrons, the ever-present randomness causes the resistance to rise as the temperature is decreased, leading to an insulating ground state. However, new evidence has emerged within the past decade indicating a transition from insulating to metallic phase in two-dimensional systems of *strongly* interacting electrons. We review earlier experiments that demonstrate the unexpected presence of a metallic phase in two dimensions, and present an overview of recent experiments with emphasis on the anomalous magnetic properties that have been observed in the vicinity of the transition.

E-mail: s.kravchenko@neu.edu; sarachik@sci.ccny.cuny.edu

Journal ref.: *Rep. Prog. Phys.* **67**, 1 (2004)

<i>Metal-insulator transition in 2D</i>	2
1 INTRODUCTION	3
2 EXPERIMENTAL RESULTS IN ZERO MAGNETIC FIELD	5
2.1 Resistance in zero magnetic field, experimental scaling, reflection symmetry	5
2.2 How universal is $\rho(T)$?	7
2.3 Critical density	12
2.4 Does weak localization survive in the presence of strong interactions?	15
3 THE EFFECT OF A MAGNETIC FIELD	18
3.1 Resistance in a parallel magnetic field	18
3.2 Scaling of the magnetoresistance; evidence for a phase transition	22
4 SPIN SUSCEPTIBILITY NEAR THE METAL-INSULATOR TRANSITION	26
4.1 Experimental measurements of the spin susceptibility	26
4.2 Effective mass and g -factor	31
4.3 Electron-electron interactions near the transition	34
5 HOW DOES ALL THIS FIT THEORY?	35
5.1 The diffusive regime: Renormalization group analysis	36
5.2 Farther from the transition (the ballistic regime)	39
5.3 Approaches not based on Fermi liquid	42
6 CONCLUSIONS	43
7 REFERENCES	45

1. INTRODUCTION

In two-dimensional electron systems, the electrons are confined to move in a plane in the presence of a random potential. According to the scaling theory of localization (Abrahams *et al* 1979), these systems lie on the boundary between high and low dimensions insofar as the metal-insulator transition is concerned. The carriers are always strongly localized in one dimension, while in three dimensions, the electronic states can be either localized or extended. In the case of two dimensions the electrons may conduct well at room temperature, but a weak logarithmic increase of the resistance is expected as the temperature is reduced. This is due to the fact that, when scattered from impurities back to their starting point, electron waves interfere constructively with their time reversed paths. While this effect is weak at high temperatures due to inelastic scattering events, quantum interference becomes increasingly important as the temperature is reduced and leads to localization of the electrons, albeit on a large length scale; this is generally referred to as “weak localization”. Indeed, thin metallic films and two-dimensional electron systems fabricated on semiconductor surfaces were found to display the predicted logarithmic increase of resistivity (Dolan and Osheroff 1979; Bishop *et al* 1980, 1982; Uren *et al* 1980), providing support for the weak localization theory.

The scaling theory does not explicitly consider the effect of the Coulomb interaction between electrons. The strength of the interactions is usually characterized by the dimensionless Wigner-Seitz radius, $r_s = 1/(\pi n_s)^{1/2} a_B$ (here n_s is the electron density and a_B is the Bohr radius in a semiconductor). In the experiments mentioned above, the Coulomb interactions are relatively weak. Indeed, these experiments are in agreement with theoretical predictions (Altshuler, Aronov and Lee 1980) that weak electron-electron interactions ($r_s \ll 1$) increase the localization even further. As the density of electrons is reduced, however, the Wigner-Seitz radius grows and the interactions provide the dominant energy of the system. No analytical theory has been developed to date in the strongly-interacting limit ($r_s \gg 1$). Finkelstein (1983, 1984) and Castellani *et al* (1984) predicted that for weak disorder and sufficiently strong interactions, a 2D system should scale towards a *conducting* state as the temperature is lowered. However, the scaling procedure leads to an increase in the effective strength of the interactions and to a divergent spin susceptibility, so that the perturbative approach breaks down as the temperature is reduced toward zero. Therefore, the possibility of a 2D metallic ground state stabilized by strong electron-electron interactions was not seriously considered.

Recent progress in semiconductor technology has enabled the fabrication of high quality 2D samples with very low randomness in which measurements can be made at very low carrier densities. The strongly-interacting regime ($r_s \gg 1$) has thus become experimentally accessible. Experiments on low-disordered 2D silicon samples (Kravchenko *et al* 1994, 1995, 1996) demonstrated that there are surprising and dramatic differences between the behaviour of strongly interacting systems at $r_s > 10$ as compared with weakly-interacting systems: with increasing electron density, one can cross from the regime where the resistance diverges with decreasing temperature (insulating behaviour) to a regime where the resistance decreases strongly with decreasing T (metallic behaviour). These results were met with great scepticism and largely overlooked until 1997, when they were confirmed in silicon MOSFETs from a different source (Popović *et al* 1997) and in other strongly-interacting 2D systems (Coleridge *et al* 1997; Hanein *et al* 1998a; Papadakis and Shayegan 1998). Moreover, it

was found (Simonian *et al* 1997b; Pudalov *et al* 1997; Simmons *et al* 1998) that in the strongly-interacting regime, an external magnetic field strong enough to polarize the electrons' spins induces a giant positive in-plane magnetoresistance[‡] and completely suppresses the metallic behaviour, thus implying that the spin state is central to the high conductance of the metallic state. This finding was in qualitative agreement with the prediction of Finkelstein and Castellani *et al* that for spin-polarized electrons, only an insulating ground state is possible in a disordered 2D system even in the presence of strong interactions. Subsequent experiments (Okamoto *et al* 1999; Kravchenko *et al* 2000b; Shashkin *et al* 2001, 2002; Vitkalov *et al* 2001b, 2002; Pudalov *et al* 2002b; Zhu *et al* 2003) have shown that there is a sharp enhancement of the spin susceptibility as the metal-insulator transition is approached; indications exist that in silicon MOSFETs, the spin susceptibility may actually diverge at some sample-independent electron density $n_\chi \approx 8 \cdot 10^{10} \text{ cm}^{-2}$.

In silicon samples with very low disorder potential, the critical density for the metal-insulator transition was found to be at or very near n_χ (Shashkin *et al* 2001a, 2002; Vitkalov *et al* 2001b, 2002), indicating that the metal-insulator transition observed in these samples is a property of a clean disorder-free 2D system, rather than being a disorder-driven transition. In such samples, the metallic and insulating regimes are divided by a temperature-independent separatrix with $\rho \approx 3h/e^2$, in the vicinity of which the resistivity displays virtually universal critical behaviour. However, in samples with relatively strong disorder, the electrons become localized at densities significantly higher than n_χ : from $1.44 \cdot 10^{11}$ to $6.6 \cdot 10^{11} \text{ cm}^{-2}$ (Prus *et al* 2002), and even as high as $1.6 \cdot 10^{12} \text{ cm}^{-2}$ (Pudalov *et al* 1999), indicating that the localization transition in these samples is driven by disorder.

We suggest that there has been a great deal of confusion and controversy caused by the fact that often no distinction has been made between results obtained in systems with relatively high disorder and those obtained for very clean samples, and also because in many experimental studies, a change in the sign of the derivative dR/dT has always been assumed to signal a metal-insulator transition. In this review, we focus our attention on results for very clean samples.

The experimental findings described above were quite unexpected. Once accepted, they elicited strong and widespread interest among theorists, with proposed explanations that included unusual superconductivity (Phillips *et al* 1998), charging/discharging of contaminations in the oxide (Altshuler and Maslov 1999), the formation of a disordered Wigner solid (Chakravarty *et al* 1999), inter-subband scattering (Yaish *et al* 2000) and many more (for a review, see Abrahams, Kravchenko and Sarachik 2001). It is now well-documented that the metallic behaviour in zero magnetic field is caused by the delocalizing effect associated with strong electron-electron interactions which overpower quantum localization. In the “ballistic regime” deep in the metallic state, the conductivity is linear with temperature and derives from coherent scattering of electrons by Friedel oscillations (Zala, Narozhny and Aleiner 2001). Closer to the transition, in the “diffusive” regime, the temperature dependence of the resistance is well described by a renormalization group analysis of the interplay of strong interactions and disorder (Punnoose and Finkelstein 2002). Within both theories (which consider essentially two limits of the same physical process) an external magnetic field quenches the delocalizing effect of interactions by aligning the spins,

[‡] The fact that the parallel magnetic field promotes insulating behaviour in strongly interacting 2D systems was first noticed by Dolgoplov *et al* (1992).

and causes a giant positive magnetoresistance. However, the metal-insulator transition itself, as well as the dramatic increase of the spin susceptibility and effective mass in its close vicinity, still lack adequate theoretical description; in this region the system appears to behave well beyond a weakly interacting Fermi liquid.

In the next three sections, we describe the main experimental results that demonstrate the unexpected presence of a metallic phase in 2D and present an overview of recent experiments with emphasis on the anomalous magnetic properties observed in the vicinity of the metal-insulator transition.

2. EXPERIMENTAL RESULTS IN ZERO MAGNETIC FIELD

2.1. Resistance in zero magnetic field, experimental scaling, reflection symmetry

The first experiments that demonstrated the unusual temperature dependence of the resistivity (Kravchenko *et al* 1994, 1995, 1996) were performed on low-disordered silicon metal-oxide-semiconductor field-effect transistors (MOSFETs) with maximum electron mobilities reaching more than $4 \cdot 10^4$ cm²/Vs, mobilities that were considerably higher than in samples used in earlier investigations. It was the very high quality of the samples that allowed access to the physics at electron densities below 10^{11} cm⁻². At these low densities, the Coulomb energy, E_C , is the dominant parameter. Estimates for Si MOSFETs at $n_s = 10^{11}$ cm⁻² yield $E_C \approx 10$ meV, while the Fermi energy, E_F , is about 0.6 meV (a valley degeneracy of two is taken into account when calculating the Fermi energy, and the effective mass is assumed to be equal to the band mass, m_b .) The ratio between the Coulomb and Fermi energies, $r^* \equiv E_C/E_F$, thus assumes values above 10 in these samples.

Figure 1 (a) shows the temperature dependence of the resistivity measured in units of h/e^2 of a high-mobility MOSFET for 30 different electron densities n_s varying from $7.12 \cdot 10^{10}$ to $13.7 \cdot 10^{10}$ cm⁻². If the resistivity at high temperatures exceeds the quantum resistance h/e^2 (the curves above the dashed red line), $\rho(T)$ increases monotonically as the temperature decreases, behaviour that is characteristic of an insulator. However, for n_s above a certain “critical” value, n_c (the curves below the “critical” curve that extrapolates to $3h/e^2$ denoted in red), the temperature dependence of $\rho(T)$ becomes non-monotonic: with decreasing temperature, the resistivity first increases (at $T > 2$ K) and then starts to decrease. At yet higher density n_s , the resistivity is almost constant at $T > 4$ K but drops by an order of magnitude at lower temperatures, showing strongly metallic behaviour as $T \rightarrow 0$.

A striking feature of the $\rho(T)$ curves shown in Figure 1 (a) for different n_s is that they can be made to overlap by applying a (density-dependent) scale factor along the T -axis. Thus, the resistivity can be expressed as a function of T/T_0 with T_0 depending only on n_s . This was demonstrated for several samples over a rather wide range of electron densities (typically $(n_c - 2.5 \cdot 10^{10}) < n_s < (n_c + 2.5 \cdot 10^{10}$ cm⁻²)) and in the temperature interval 0.2 to 2 K. The results of this scaling are shown in Fig. 1 (b), where ρ is plotted as a function of T/T_0 . One can see that the data collapse onto two separate branches, the upper one for the insulating side of the transition and the lower one for the metallic side. The thickness of the lines is largely governed by the noise within a given data set, attesting to the high quality of the scaling.

The procedure used to bring about the collapse and determine T_0 for each n_s was the following. No power law dependence was assumed *a priori* for T_0 versus $(n_s - n_c)$; instead, the $\rho(T)$ curves were successively scaled along the T -axis to coincide: the

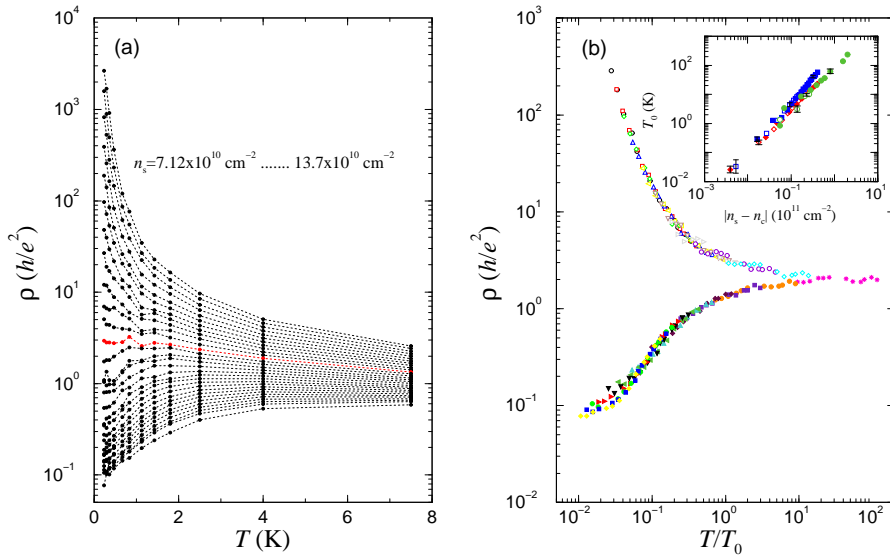


Figure 1. (a): temperature dependence of the $B = 0$ resistivity in a dilute low-disordered Si MOSFET for 30 different electron densities n_s ranging from 7.12 to $13.7 \cdot 10^{10} \text{ cm}^{-2}$. (b): resistivity versus T/T_0 , with $T_0(n_s)$ chosen to yield scaling with temperature. The inset shows the scaling parameter, T_0 , versus the deviation from the critical point, $|n_s - n_c|$; data are shown for silicon MOSFETs obtained from three different wafers. Open symbols correspond to the insulating side and closed symbols to the metallic side of the transition. From Kravchenko *et al* (1995).

second “insulating” curve from the top was scaled along the T -axis to coincide with the top-most curve and the corresponding scaling factor was recorded, then the third, and so on, yielding the upper curve in Fig. 1 (b) (designated by open symbols). The same procedure was applied on the metallic side of the transition starting with the highest-density curve, giving the lower curve in Fig. 1 (b) (shown as closed symbols). A quantitative value was assigned to the scaling factor to obtain T_0 for the insulating curves by using the fact that the resistivity of the most insulating (lowest n_s) curve was shown (Mason *et al*, 1995) to exhibit the temperature dependence characteristic of hopping in the presence of a Coulomb gap: $\rho = \rho_0 \exp[(T_0/T)^{1/2}]$ (Efros and Shklovskii 1975). T_0 was determined on the metallic side using the symmetry between metallic and insulating curves, as described in more detail in Kravchenko *et al* (1995). For all samples studied, this scaling procedure yields a power law dependence of T_0 on $|\delta_n| \equiv |n_s - n_c|$ on both sides of the transition: $T_0 \propto |\delta_n|^\beta$ with the average power $\beta = 1.60 \pm 0.1$ for the insulating side and 1.62 ± 0.1 for the metallic side of the transition; this common power law can be clearly seen in the inset to Fig. 1 (b), where for each sample the open (insulating side) and filled (metallic side) symbols form a single line. The same power law was later observed by Popović (1997) in silicon samples from another source, thus establishing its universality and supporting the validity of the scaling analysis.

Simonian *et al* (1997a) noted that the metallic and insulating curves are reflection-symmetric in the temperature range between approximately 300 mK and 2 K. In

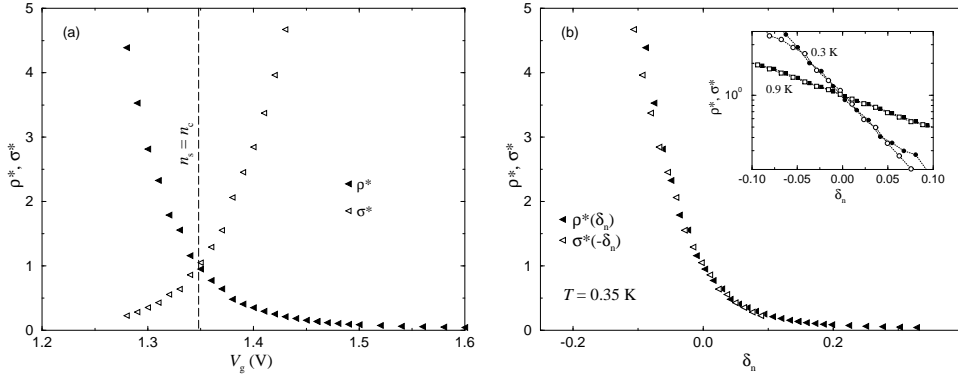


Figure 2. (a) For a silicon MOSFET, the normalized resistivity, ρ^* , and normalized conductivity, σ^* , as a function of the gate voltage, V_g , at $T = 0.35$ K. Note the symmetry about the line $n_s = n_c$. The electron density is given by $n_s = (V_g - 0.58\text{V}) \cdot 1.1 \cdot 10^{11} \text{ cm}^{-2}$. (b) To demonstrate this symmetry explicitly, $\rho^*(\delta_n)$ (closed symbols) and $\sigma^*(-\delta_n)$ (open symbols) are plotted as a function of $\delta_n \equiv (n_s - n_c)/n_c$. Inset: $\rho^*(\delta_n)$ (closed symbols) and $\sigma^*(-\delta_n)$ (open symbols) versus δ_n at $T = 0.3$ K and $T = 0.9$ K, the lowest and highest measured temperatures. From Simonian *et al* (1997a).

Fig. 2 (a), the normalized resistivity, $\rho^* \equiv \rho/\rho(n_c)$, is shown as a function of the gate voltage, V_g , together with the normalized conductivity, $\sigma^* \equiv 1/\rho^*$; the apparent symmetry about the vertical line corresponding to the critical electron density can be clearly seen. Fig. 2 (b) demonstrates that the curves can be mapped onto each other by reflection, *i.e.*, $\rho^*(\delta_n)$ is virtually identical to $\sigma^*(-\delta_n)$. This mapping holds over a range of temperature from 0.3 K to 0.9 K; however, the range $|\delta_n|$ over which it holds decreases as the temperature is decreased: for example, at $T = 0.9$ K, ρ^* and σ^* are symmetric for $|\delta_n| < 0.1$, while at $T = 0.3$ K, they are symmetric only for $|\delta_n| < 0.05$ (see inset to Fig. 2 (b)). Similar symmetry was later reported by Popović *et al* (1997) and Simmons *et al* (1998). This implies that there is a simple relation between the mechanism for conduction on opposite sides in the vicinity of the transition; the data bear a strong resemblance to the behaviour found by Shahar *et al* (1996) for the resistivity near the transition between the quantum Hall liquid and insulator, where it has been attributed to charge-flux duality in the composite boson description. It was argued by Dobrosavljević *et al* (1997) that both the scaling and reflection symmetry are consequences of a simple analysis assuming that a $T = 0$ quantum critical point describes the metal-insulator transition.

2.2. How universal is $\rho(T)$?

The temperature dependence of $\rho(T)$ is very similar for clean silicon MOSFETs. As an example, Fig. 3 shows the resistivity as a function of temperature of three low-disordered samples obtained from different sources. The behaviour is quantitatively similar in the critical region in the vicinity of the “separatrix”, which is the horizontal curve for which the resistivity is independent of temperature. In all samples, the

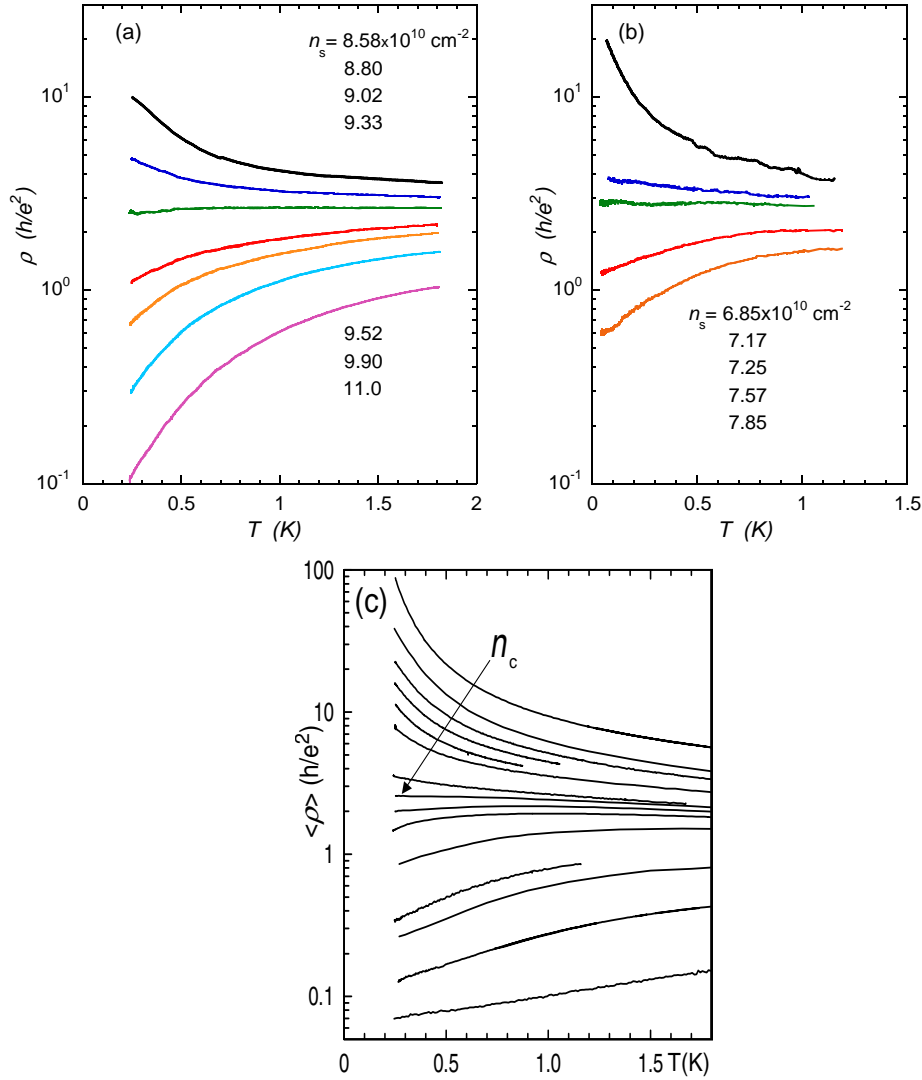


Figure 3. Universal behaviour in ultra-clean silicon MOSFETs: the resistivity versus temperature in three samples from different sources. Note that the resistivities are essentially the same at the separatrices for all samples even though their critical densities are different. (a) high-mobility sample provided by V M Pudalov (graph adopted from Sarachik and Kravchenko 1999), (b) sample fabricated by Heemskerk and Klapwijk (1998) (adopted from Kravchenko and Klapwijk 2000a) and (c) sample of Heemskerk and Klapwijk but from a different wafer (graph adopted from Jaroszyński *et al* 2002). Electron densities in (c) vary from 8.55 to $14 \cdot 10^{10} \text{ cm}^{-2}$ (top to bottom).

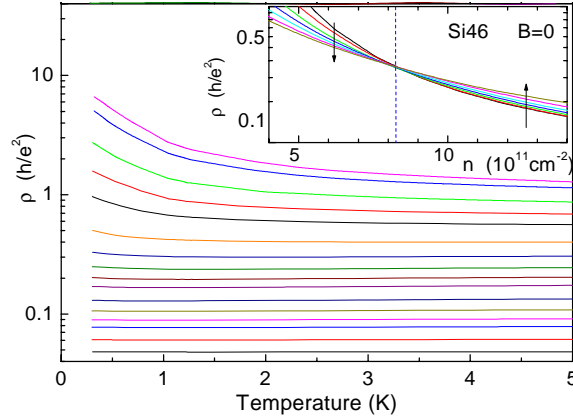


Figure 4. Resistivity versus temperature of a very disordered silicon MOSFET. Note that the vertical scale is similar to Fig. 3. The electron densities are (in units of 10^{11} cm^{-2}): 3.85, 4.13, 4.83, 5.53, 6.23, 7.63, 9.03, 10.4, 11.8, 13.2, 16.0, 18.8, 21.6, 24.4, 30.0 and 37. Adopted from Pudalov *et al* (2001). Even though there is an apparent crossing point on the $\rho(n_s)$ isotherms (see the inset), the temperature dependence of the resistivity does not resemble the critical behaviour seen in low-disordered samples.

separatrix is remarkably flat at temperatures below 1 K \ddagger , and the resistivity is essentially the same numerically at slightly less than $3h/e^2$. The curves below the separatrix exhibit strongly metallic temperature dependence ($d\rho/dT > 0$) with no low- T saturation down to the lowest temperature (40 mK or lower; see Fig.3 (b)); the drop in resistivity reaches as much as a factor of 10 for the bottom curve in Fig.3 (a). Alternative methods used to determine the critical electron density in low-disordered samples yield the same value as the density for the separatrix (see sec. 2.3). It is important to note that the separatrix in ultra-clean samples represents the “upper limit” of the resistivity for which metallic behaviour (as characterized by $d\rho/dT > 0$) can exist: metallic $\rho(T)$ has never been observed in any 2D samples at resistivities above $\approx 3h/e^2$, in quantitative agreement with the predictions of the renormalization group theory (see sec.5.1).

In more disordered samples, however, the behaviour of the resistivity is very different. Even though the $\rho(n_s)$ isotherms apparently cross at some electron density (see the inset to Fig.4), the temperature dependence of the resistivity does not resemble the critical behaviour seen in low-disordered samples. An example of $\rho(T)$ curves in a disordered sample is shown in Fig.4. The sample is insulating at electron densities up to $\sim 8 \cdot 10^{11} \text{ cm}^{-2}$ which is an order of magnitude higher than the critical density in low-disordered samples. The metallic temperature dependence of the resistance visible at higher n_s does not exceed a few percent (compared to a factor of 10 in low-disordered samples). Most importantly, the density corresponding to the crossing point shown in the inset to Fig.4 does not coincide with the critical density determined by other methods discussed in the next subsection.

A metal-insulator transition similar to that seen in clean silicon MOSFETs has also been observed in other low-disordered, strongly-interacting 2D systems: p -

\ddagger At $T > 2$ K, the resistivity of the separatrix slowly decreases with increasing temperature, as can be seen in Fig. 1, where $\rho(T)$ curves are shown in a much wider temperature interval.

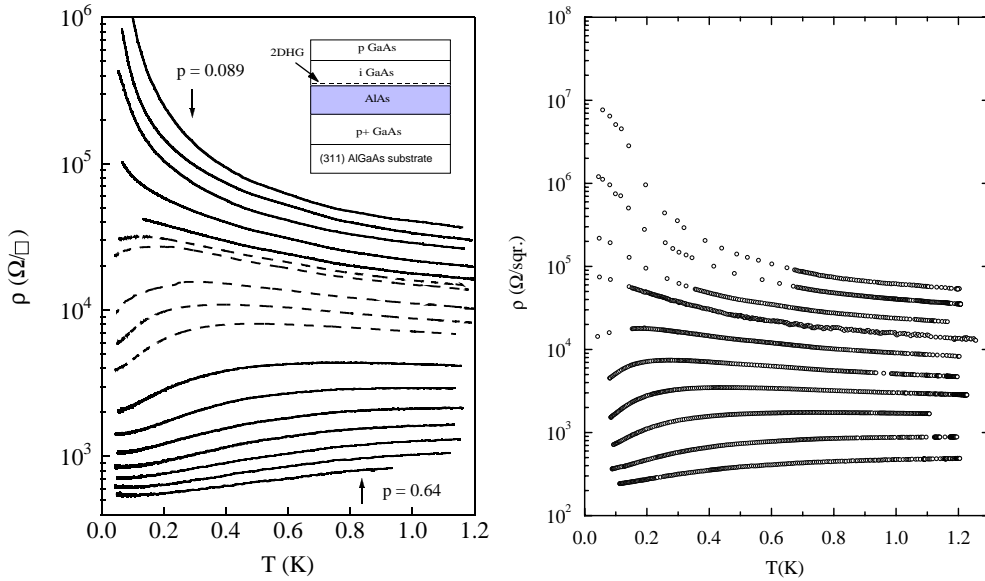


Figure 5. For low-disordered 2D hole systems in p -GaAs/AlGaAs, the resistivity per square is shown as a function of temperature for $B = 0$ at various fixed hole densities, p . Left hand panel: ISIS (inverted semiconductor-insulator-semiconductor) structure with hole densities (from top to bottom) $p = 0.89, 0.94, 0.99, 1.09, 1.19, 1.25, 1.30, 1.50, 1.70, 1.90, 2.50, 3.20, 3.80, 4.50, 5.10, 5.70$ and $6.40 \cdot 10^{10} \text{ cm}^{-2}$. The inset shows a schematic diagram of the ISIS structure: The carriers are accumulated in an undoped GaAs layer situated on top of an undoped AlAs barrier, grown over a p^+ conducting layer which serves as a back-gate; the hole density, p , is varied by applying a voltage to the back gate. From Hanein *et al* (1998a). Right hand panel: Temperature dependence of ρ in an ultra high mobility p -type GaAs/AlGaAs heterostructure at $p = 0.48, 0.55, 0.64, 0.72, 0.90, 1.02, 1.27, 1.98, 2.72$ and $3.72 \cdot 10^{10} \text{ cm}^{-2}$ (from top to bottom). From Yoon *et al* (1999).

type SiGe heterostructures (Coleridge *et al* 1997), GaAs/AlGaAs heterostructures (Hanein *et al* 1998a; Yoon *et al* 1999; Mills *et al* 1999; Noh *et al* 2002 and others) and AlAs heterostructures (Papadakis and Shayegan 1998). It is difficult to make a direct comparison of the resistivity observed in different material systems because the temperature scales are different, since the Coulomb and Fermi energies depend on the effective mass and carrier density. For example, the characteristic temperature below which the metallic decrease in the resistivity occurs in p -type GaAs/AlGaAs samples is about ten times smaller than in silicon MOSFETs. On the other hand, the values of the resistivity are quite similar in the two systems. In Fig. 5, the resistivity is plotted as a function of temperature for two p -type GaAs/AlGaAs samples produced using different technologies. The data shown in the left hand panel were obtained by Hanein *et al* (1998a) for an inverted semiconductor-insulator-semiconductor (ISIS) structure with maximum mobility of $\mu_{\text{max}} = 1.5 \cdot 10^5 \text{ cm}^2/\text{Vs}$, while the right-hand panel shows $\rho(T)$ measured by Yoon *et al* (1999) on a p -type GaAs/AlGaAs heterostructure with peak mobility by a factor of five higher ($7 \cdot 10^5 \text{ cm}^2/\text{Vs}$). The interaction parameter, r_s , changes between approximately 12 and 32 for the left hand

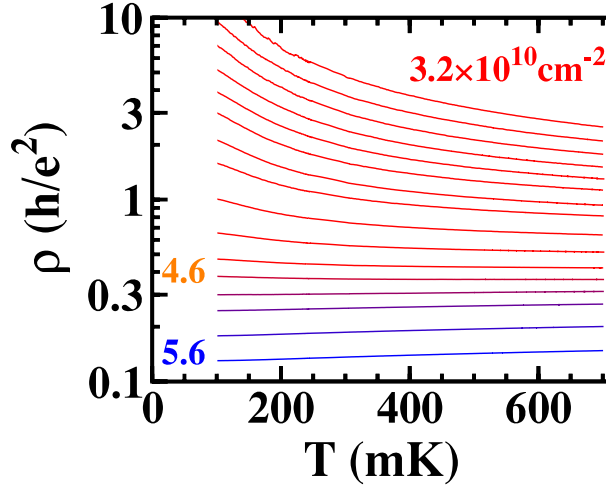


Figure 6. The resistivity as a function of temperature for a disordered p -type GaAs/AlGaAs heterostructure at hole densities $p = 3.2 - 5.6 \cdot 10^{10} \text{ cm}^{-2}$. From Simmons *et al* (2000).

plot and from 16 to 44 for the right hand plot||. In spite of the difference in the sample quality and range of densities, the dependence of $\rho(T)$ on temperature is almost the same for the two samples. The main features are very similar to those found in silicon MOSFETs: when the resistivity at “high” temperatures exceeds the quantum resistance, h/e^2 (*i.e.*, at hole densities below some critical value, p_c), the $\rho(T)$ curves are insulating-like in the entire temperature range; for densities just above p_c , the resistivity shows insulating-like behaviour at higher temperatures and then drops by a factor of 2 to 3 at temperatures below a few hundred mK; and at yet higher hole densities, the resistivity is metallic in the entire temperature range. Note that the curves that separate metallic and insulating behaviour have resistivities that increase with decreasing temperature at the higher temperatures shown; this is quite similar to the behaviour of the separatrix in silicon MOSFETs when viewed over a broad temperature range (see Fig. 1 (a)). However, below approximately 150 mK, the separatrix in p -type GaAs/AlGaAs heterostructures is independent of temperature (Hanein *et al*, 1998b), as it is in Si MOSFETs below approximately 2 K. The resistivity of the separatrix in both systems extrapolates to $2 - 3 h/e^2$ as $T \rightarrow 0$, even though the corresponding carrier densities are very different.

As in the case of highly disordered silicon MOSFETs, no critical behaviour of resistance is observed in disordered GaAs/AlGaAs heterostructures. An example is shown in Fig. 6 where the temperature dependence of the resistivity at $B = 0$ is plotted for hole densities $p = 3.2 - 5.6 \cdot 10^{10} \text{ cm}^{-2}$. Monotonic localized behaviour is observed even when the “high-temperature” resistivity lies well below h/e^2 , at carrier densities up to $4.6 \cdot 10^{10} \text{ cm}^{-2}$; both samples shown in the previous figure would be in the deeply metallic regime at this hole density. Above this density, the decrease in resistivity with decreasing temperature is very small (about 10% in the temperature interval 0.7 to 0.1 K).

|| These r_s values were calculated assuming that the effective mass is independent of density and equal to $0.37 m_e$, where m_e is the free-electron mass.

As indicated by the experimental results presented above, the $\rho(T)$ curves are nearly universal in the vicinity of the metal-insulator transition, but only in samples with very weak disorder potential. The strength of the disorder is usually characterized by the maximum carrier mobility, μ_{\max} . In general, the higher the maximum mobility (*i.e.* the lower the disorder), the lower the carrier density at which the localization transition occurs. This was shown empirically by Sarachik (2002) to hold over a broad range (five decades in density) for all materials studied: the critical density follows a power law dependence on peak mobility (or scattering rate). However, the data exhibit some scatter, and the correlation is not exact. Thus, for example, the peak hole mobilities in samples used by Hanein *et al* (1998a) and Simmons *et al* (1998) are similar, while the localization transition occurs in the latter at a value of p several times higher than the former. This may be due to sample imperfections (*e.g.*, a slightly inhomogeneous density distribution), which are important at low carrier densities, while the maximum mobility is reached at relatively high carrier densities and may therefore be relatively insensitive to such effects.

A better indicator of the strength of the disorder potential near the MIT is how low the carrier density is at which the localization transition occurs. In silicon MOSFETs, the experimental results obtained to date suggest that the resistivity near the transition approaches universal behaviour for samples in which the transition to a strongly localized state occurs at $n_s < 1 \cdot 10^{11} \text{ cm}^{-2}$. (In p -type GaAs/AlGaAs heterostructures, the corresponding density separating universal and non-universal behaviour appears to be about an order of magnitude lower, although the data are currently insufficient to determine the value reliably.) Below, we will argue that the “universal” metal-insulator transition in very clean samples is not driven by disorder but by some other mechanism, possibly of magnetic origin. In contrast, the transition is not universal in more disordered samples and is presumably due to Anderson localization, which is strong enough to overpower the metallic behaviour at low densities.

2.3. Critical density

To verify whether or not the separatrix corresponds to the critical density, an independent determination of the critical point is necessary: comparison of values obtained using different criteria provides an experimental test of whether or not a true MIT exists at $B = 0$. One obvious criterion, hereafter referred to as the “derivative criterion”, is a change in sign of the temperature derivative of the resistivity, $d\rho/dT$; this is the criterion often used to identify the MIT. A positive (negative) sign of the derivative at the lowest achievable temperatures is empirically associated with a metallic (insulating) phase. A weakness of this criterion is that it requires extrapolation to zero temperature. A second criterion can be applied based on an analysis of a temperature-independent characteristic, namely, the localisation length L extrapolated from the insulating phase. These two methods have been applied to low-disordered silicon MOSFETs by Shashkin *et al* (2001b) and Jaroszyński *et al* (2002).

As mentioned earlier, the temperature dependence of the resistance deep in the insulating phase obeys the Efros-Shklovskii variable-range hopping form (Mason *et al* 1995); on the other hand, closer to the critical electron density at temperatures that are not too low, the resistance has an activated form $\rho \propto e^{E_a/k_B T}$ (Pepper *et al* 1974; Pudalov *et al* 1993; Shashkin *et al* 1994) due to thermal activation to the mobility

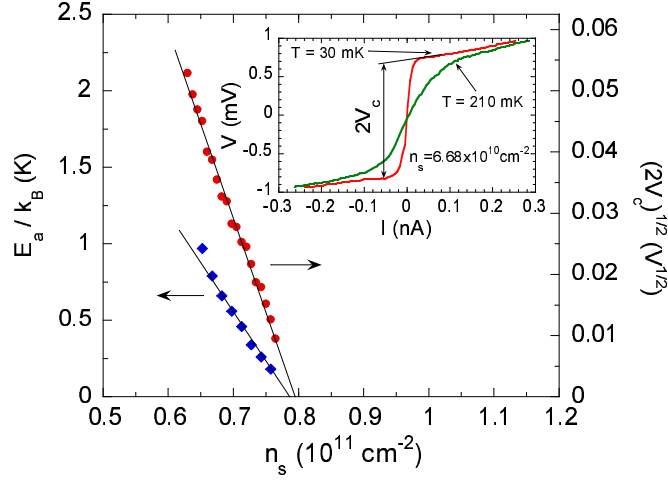


Figure 7. Activation energy (diamonds) and square root of the threshold voltage (circles) versus electron density in zero magnetic field in a low-disordered silicon MOSFET. The inset shows current-voltage characteristics recorded at ≈ 30 and 210 mK, as labelled; note that the threshold voltage is essentially independent of temperature. From Shashkin *et al* (2001b).

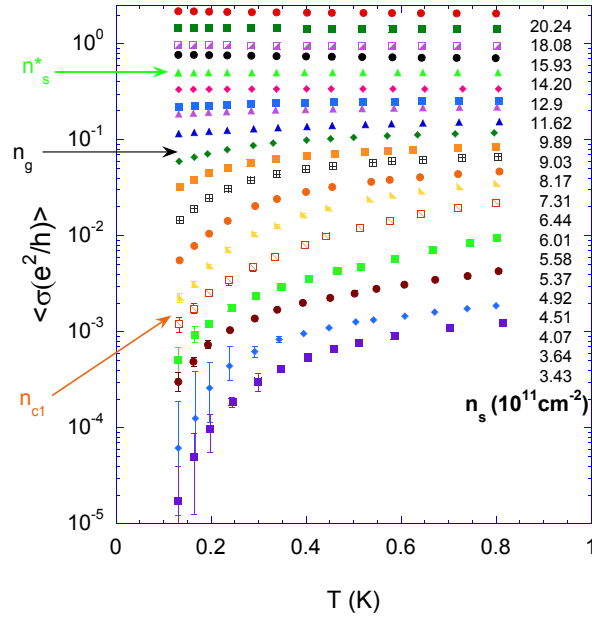


Figure 8. Conductivity versus temperature for different n_s in a highly disordered silicon MOSFET. (The error bars show the size of the fluctuations of the conductivity with time.) The critical electron densities obtained by the derivative and localization length criteria (n_s^* and n_{c1} , correspondingly) are marked by arrows. n_g is the density corresponding to the onset of glassy behaviour; see text. The figure is adopted from Bogdanovich and Popović (2002).

edge. Fig. 7 shows the activation energy E_a as a function of the electron density (diamonds); the data can be approximated by a linear function which yields, within the experimental uncertainty, the same critical electron density as the “derivative criterion”.

The critical density can also be determined by studying the nonlinear current-voltage $I - V$ characteristics on the insulating side of the transition. A typical low-temperature $I - V$ curve is close to a step-like function: the voltage rises abruptly at low current and then saturates, as shown in the inset to Fig. 7; the magnitude of the step is $2V_c$. The curve becomes less sharp at higher temperatures, yet the threshold voltage, V_c , remains essentially unchanged. Closer to the MIT, the threshold voltage decreases, and at $n_s = n_{c1} = 0.795 \cdot 10^{11} \text{ cm}^{-2}$, the $I - V$ curve is strictly linear (Shashkin *et al* 2001b). According to Polyakov and Shklovskii (1993) and Shashkin *et al* (1994), the breakdown of the localized phase occurs when the localized electrons at the Fermi level gain enough energy to reach the mobility edge in an electric field, V_c/d , over a distance given by the localization length, L , which is temperature-independent:

$$eV_c(n_s) L(n_s)/d = E_a(n_s)$$

(here d is the distance between the potential probes). The dependence of $V_c^{1/2}(n_s)$ near the MIT is linear, as shown in Fig. 7 by closed circles, and its extrapolation to zero threshold value again yields approximately the same critical electron density as the two previous criteria. The linear dependence $V_c^{1/2}(n_s)$, accompanied by linear $E_a(n_s)$, signals the localization length diverging near the critical density: $L(n_s) \propto 1/(n_c - n_s)$.

These experiments indicate that in low-disordered samples, the two methods — one based on extrapolation of $\rho(T)$ to zero temperature and a second based on the behaviour of the temperature-independent localization length — give the same critical electron density: $n_c \approx n_{c1}$. This implies that the separatrix remains “flat” (or extrapolates to a finite resistivity) at zero temperature. Since one of the methods is independent of temperature, this equivalence supports the existence of a true $T = 0$ MIT in low-disordered samples in zero magnetic field.

In contrast, we note that in highly-disordered samples, the localization length method yields a critical density noticeably lower than the derivative criterion. Figure 8 shows the (time-averaged) conductivity $\langle\sigma\rangle$ as a function of T for different n_s . $d\langle\sigma\rangle/dT$ changes sign at electron density $n_s^* = 12.9 \cdot 10^{11} \text{ cm}^{-2}$. The activation energy, however, vanishes at $n_{c1} \approx 5.2 \cdot 10^{11} \text{ cm}^{-2}$, which is more than a factor of two lower than n_s^* : at densities between these two values, the resistivity does not diverge as $T \rightarrow 0$, even though it exhibits an insulating-like temperature dependence. Thus, these two different methods yield different “critical densities” for a sample with strong disorder. Moreover, from the study of low-frequency resistance noise in dilute silicon MOSFETs, Bogdanovich and Popović (2002) and Jaroszyński *et al* (2002) have found that the behaviour of several spectral characteristics indicates a dramatic slowing down of the electron dynamics at a well-defined electron density n_g , which they have interpreted as an indication of a (glassy) freezing of the 2D electron system. In low-disordered samples, n_g nearly coincides with n_c , while in highly-disordered sample, n_g lies somewhere between n_{c1} and n_s^* , as indicated in Fig. 8. The width of the glass phase ($n_{c1} < n_s < n_g$) thus strongly depends on disorder, becoming extremely narrow (or perhaps even vanishing) in low-disordered samples. The strong dependence on disorder of the width of the metallic glass phase is consistent with predictions of the model of interacting electrons near a disorder-driven metal-insulator transition

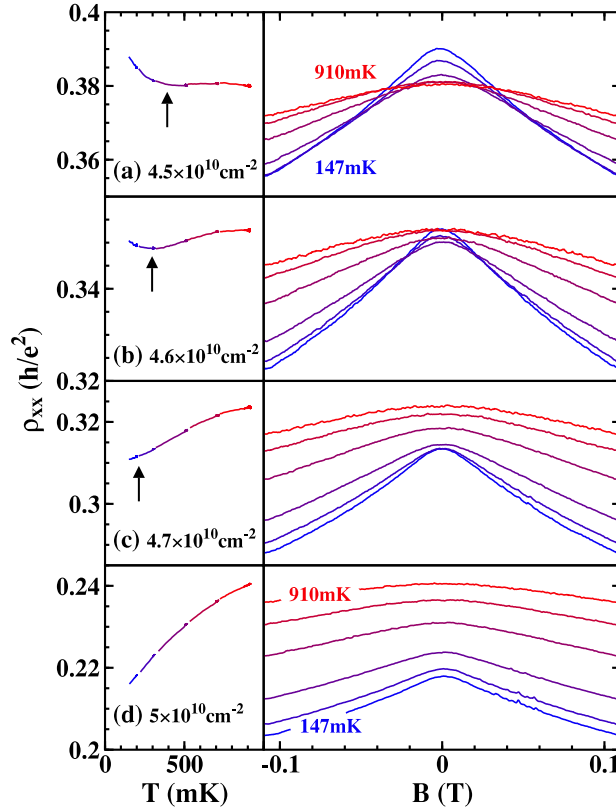


Figure 9. (a-d) The left hand panels show data for the resistivity versus temperature at $B = 0$ in a disordered p -type GaAs/AlGaAs quantum well, illustrating the transition from insulating to metallic behaviour as the density increases. The right hand panels show the corresponding magnetoresistance traces for temperatures of 147, 200, 303, 510, 705, and 910 mK. From Simmons *et al* (2000).

(Pastor and Dobrosavljević 1999). These observations all suggest that the origin of the metal-insulator transition is different in clean and strongly-disordered samples.

2.4. Does weak localization survive in the presence of strong interactions?

The theory of weak localization was developed for noninteracting systems, and it was not *a priori* clear whether it would work in the presence of strong interactions. In 2000, Simmons *et al* studied transport properties of a dilute modulation-doped p -type GaAs/AlGaAs quantum well and observed a temperature-dependent negative magnetoresistance, consistent with the suppression of the coherent backscattering by the perpendicular magnetic field. Magnetoresistance curves obtained by Simmons *et al* are plotted in the right hand panel of Fig. 9. A characteristic peak develops in the resistivity at $B = 0$ as the temperature is decreased, signalling that the weak localization is still present at p as low as $4.5 \cdot 10^{10} \text{ cm}^{-2}$, corresponding to the interaction parameter $r_s \sim 15$. Simmons *et al* successfully fitted their

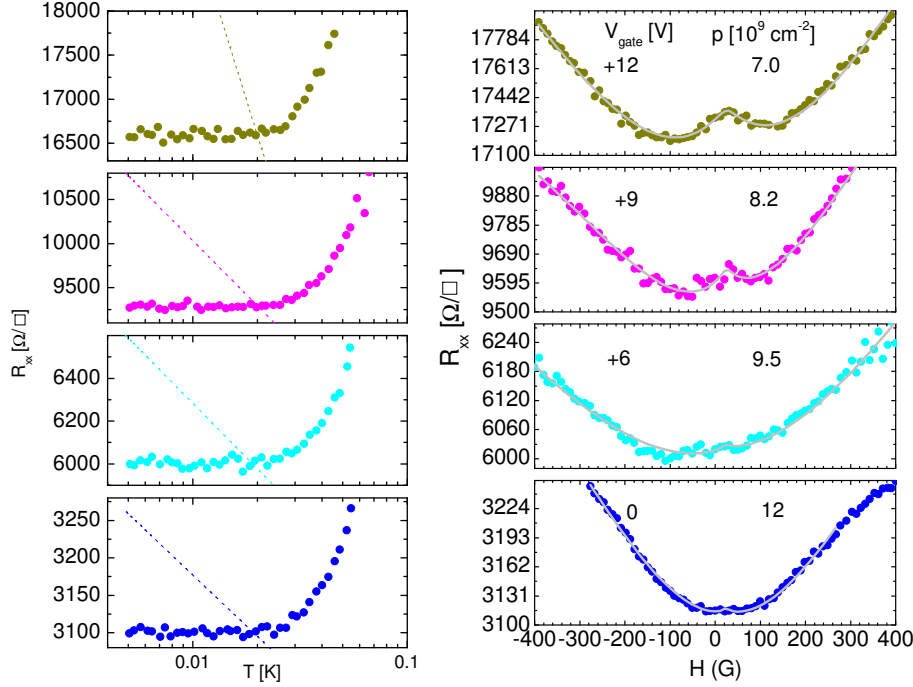


Figure 10. The left hand panels show resistance per square as a function of temperature for 2D holes in an ultra-clean GaAs/AlGaAs heterostructure for various values of the gate bias. The right hand panels show the variation of longitudinal resistance with perpendicular magnetic field for the same sample at various gate biases. The solid grey lines represent the fit described in the text. From Mills *et al* (2001).

magnetoresistance data by the Hikami-Larkin formula (Hikami *et al* 1980)

$$\Delta\sigma = -\frac{e^2}{\pi h} \left[\Psi \left(\frac{1}{2} + \frac{\tau_B}{\tau} \right) - \Psi \left(\frac{1}{2} + \frac{\tau_B}{\tau_\phi} \right) \right], \quad (1)$$

and obtained reasonable values of the phase-breaking time, $\tau_\phi \sim 10$ to 30 ps, in the temperature interval 1 to 0.15 K (here τ is the elastic scattering time, Ψ is the Digamma function, $\tau_B = \hbar/4eB_\perp D$, and D is the diffusion coefficient). Weak negative magnetoresistance was also observed by Brunthaler *et al* (2001) in silicon MOSFETs at electron densities down to $1.5 \cdot 10^{11} \text{ cm}^{-2}$, although they found values of τ_ϕ that were about an order of magnitude shorter than those expected theoretically, $\tau_\phi \sim \sigma \hbar^2 / e^2 k_B T$.

However, the agreement with non-interacting theory breaks down at higher interaction strengths. Mills *et al* (2001) studied *p*-type GaAs/AlGaAs heterostructures of much higher quality which remained metallic down to $p \approx 3 \cdot 10^9 \text{ cm}^{-2}$ (corresponding to $r_s \sim 60$ provided the effective mass does not change), and found the coherent backscattering to be almost completely suppressed at these ultra-low hole densities. In the right hand panel of Fig. 10, the magnetoresistance traces are shown at $T \approx 9$ mK for four different carrier densities. The width of the characteristic peak at $B_\perp = 0$, visible in the top two curves, is approximately as expected from the theory,

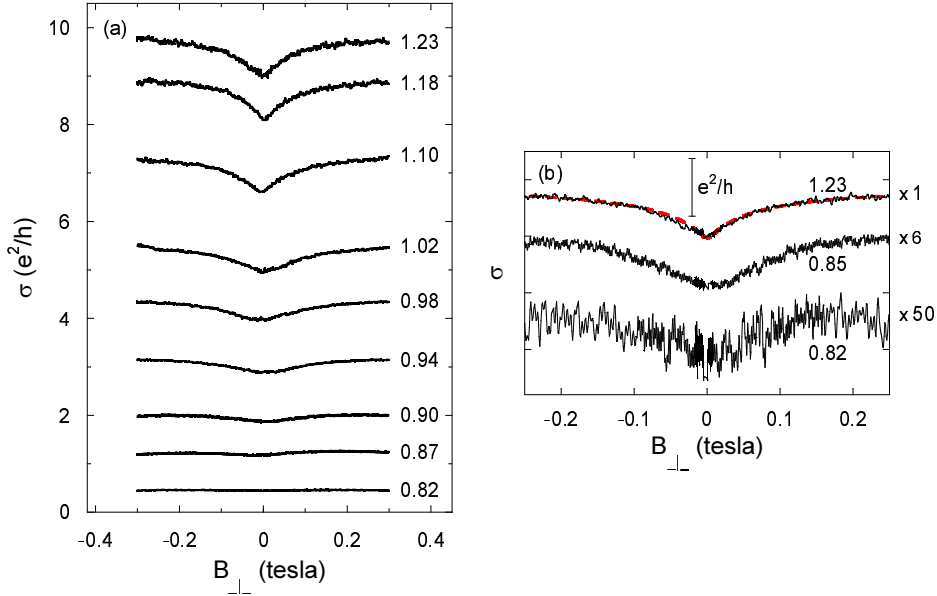


Figure 11. Longitudinal magnetoconductivity of a low-disordered silicon MOSFET in a weak perpendicular magnetic field at $T = 42$ mK for a range of electron densities indicated near each curve in units of 10^{11} cm^{-2} . The curves in (b) are vertically shifted and the two lowest curves are multiplied by 6 (the middle one) and 50 (the lower one). The thick dashed line in (b) is a fit by Eq. 1 with $b = 0.6$ and $\tau_\phi = 30$ ps. From Rahimi *et al* (2003).

but its magnitude is about a factor of 30 smaller than expected. At slightly higher p (the two bottom curves), the peak is not seen at all.

In principle, the strong disagreement between the expected and measured peak magnitudes might be due to the fact that the theory for coherent backscattering is not applicable to a system with resistivity of the order of h/e^2 . However, this is not the source of the disagreement, as the resistivity in the experiments of Mills *et al* (2001) is in the same range as in the experiments of Simmons *et al* (2000) (*cf* Figs. 9 and 10). Therefore the suppression of the peak is apparently related to stronger interactions (higher r_s) in the Mills *et al* samples rather than to high values of ρ .

The left hand panel of Fig. 10 shows the temperature dependence of the $B = 0$ resistance in the ultra low density sample of Mills *et al* over the temperature range 5 to 100 mK. The dashed lines show the expected corrections to the resistivity caused by weak localization calculated using the equation $\Delta\sigma(T) = b e^2/h \ln(\tau_\phi/\tau)$, where b is a constant expected to be universal and equal to $1/\pi$. The calculated dependence is clearly at variance with the measurements; rather, at very low temperatures, the resistance becomes nearly constant. Fitting the theoretical expression to the experimental data, Mills *et al* found that the upper limits for b are from one to nearly two orders of magnitude smaller than the $b = 1/\pi$ expected from the theory.

The disappearance of weak localization corrections near the MIT has also been observed by Rahimi *et al* (2003) in low-disordered silicon MOSFETs. The results are shown in Fig. 11. At higher n_s (the upper curves in Fig. 11 (a)), the characteristic dip is observed in the magnetoconductance at zero magnetic field. As follows from Eq. 1,

the magnitude of the dip is expected to be equal to $(b e^2 g_v / h) \ln(\tau_\phi / \tau)$, and should therefore exhibit a weak (double-logarithmic) increase as the average conductivity decreases provided the variations in electron density are small, as they are in this case. This is not what is observed in the experiment: as one approaches the transition, the magnitude of the dip decreases sharply, and at the critical electron density (the lowest curve in Fig. 11 (a)), the dip is no longer seen on the scale of this figure. However, the shape of the magnetoconductivity does not change significantly with decreasing n_s as illustrated by the middle curve in Fig. 11 (b), which shows $\sigma(B_\perp)$ multiplied by six ($n_s = 0.85 \cdot 10^{11} \text{ cm}^{-2}$) to make it quantitatively similar to the upper curve. This similarity demonstrates that the functional form of the $\sigma(B_\perp)$ dependence, described by the expression in square brackets in Eq. 1, does not change noticeably as the density is reduced from $1.23 \cdot 10^{11}$ to $0.85 \cdot 10^{11} \text{ cm}^{-2}$; instead, it is the magnitude of the effect that rapidly decreases upon approaching the MIT. At yet lower density, $n_s = 0.82 \cdot 10^{11} \text{ cm}^{-2}$, the magnitude of the dip does not exceed 2% of that for $n_s = 1.23 \cdot 10^{11} \text{ cm}^{-2}$ (compare the upper and the lower curves in Fig. 11 (b)).

It may seem surprising that a change in n_s by only a factor of 1.5 (from $n_s = 1.23 \cdot 10^{11}$ to $n_s = 0.82 \cdot 10^{11} \text{ cm}^{-2}$) results in such a dramatic suppression of the quantum localization. It is interesting to note in this connection that the experimental data on silicon MOSFETs described in sections 4.2 and 4.3 reveal a sharp increase of the effective mass in the same region of electron densities where the suppression of the weak localization is observed. Due to the strong renormalization of the effective mass, the ratio between the Coulomb and Fermi energies, $r^* = 2 r_s (m^* / m_b)$, grows much faster than $n_s^{-1/2}$ reaching values greater than 50 near the critical density.

The apparent absence of localization at and just above the critical density may account for the existence of a flat separatrix at $n_s = n_c$ (see Fig. 3). If the localization were present, the temperature-independent curve would require that the temperature dependence of ρ due to localization be cancelled exactly over a wide temperature range by a temperature dependence of opposite sign due to interactions, a coincidence which seems very improbable for two unrelated mechanisms. Note that at resistivity levels of order or greater than h/e^2 , the quantum corrections to the resistivity are expected to be very strong and cannot be easily overlooked. The calculated temperature dependence of the resistivity, expected for non-interacting electrons (Abrahams *et al* 1979), is shown in Fig.12 by the dashed curve: at 100 mK, quantum localization is expected to cause a factor of more than 30 increase in resistivity, in strong contradiction with the experiment which shows it to be constant within $\pm 5\%$.

3. THE EFFECT OF A MAGNETIC FIELD

3.1. Resistance in a parallel magnetic field

In ordinary metals, the application of a parallel magnetic field (B_\parallel) does not lead to any dramatic changes in the transport properties: if the thickness of the 2D electron system is small compared to the magnetic length, the parallel field couples largely to the electrons' spins while the orbital effects are suppressed. Only weak corrections to the conductivity are expected due to electron-electron interactions (Lee and Ramakrishnan 1982, 1985). It therefore came as a surprise when Dolgoplov *et al* (1992) observed a dramatic suppression of the conductivity in dilute Si MOSFETs by a parallel in-plane magnetic field B_\parallel . The magnetoresistance in a parallel field was studied in detail by Simonian *et al* (1997b) and Pudalov *et al* (1997), also in Si

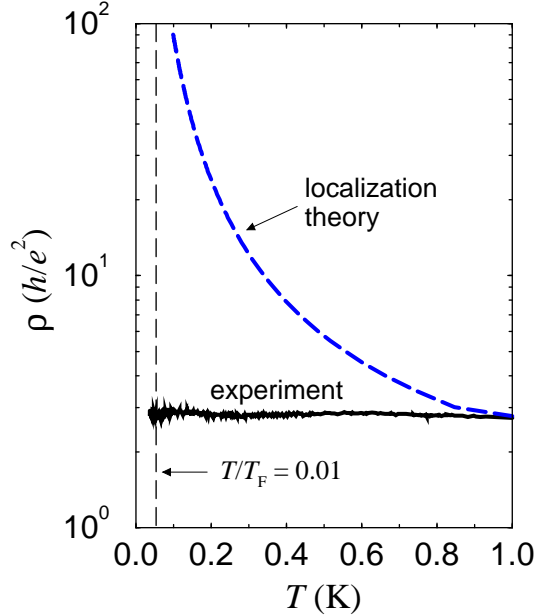


Figure 12. Resistivity at the separatrix in a low-disordered silicon MOSFET as a function of temperature (the solid curve) compared to that calculated from the one-parameter scaling theory using $\frac{d \ln \rho(L_\phi)}{d \ln L_\phi} = -\beta(\rho)$ (here $L_\phi \propto \rho^{-\gamma} T^{-p/2}$ is the phase-breaking length, $\beta(\rho)$ is the scaling function approximated by $\beta(\rho) = -\ln(1 + a\rho)$ following Altshuler *et al* (2000), $a = 2/\pi$, ρ is measured in units of h/e^2 , and p and γ are constants equal to 3 and 0.5 respectively). As the dashed line shows, the resistivity of a “conventional” (noninteracting) 2D system should have increased by a factor of more than 30 when the temperature has been reduced to 100 mK. From Kravchenko and Klapwijk (2000a).

MOSFETs. In the left hand part of Fig. 13, the resistivity is shown as a function of parallel magnetic field at a fixed temperature of 0.3 K for several electron densities. The resistivity increases sharply as the magnetic field is raised, changing by a factor of about 4 at the highest density shown and by more than an order of magnitude at the lowest density, and then saturates and remains approximately constant up to the highest measuring field, $B_{\parallel} = 12$ tesla. The magnetic field where the saturation occurs, B_{sat} , depends on n_s , varying from about 2 tesla at the lowest measured density to about 9 tesla at the highest. The metallic conductivity is suppressed in a similar way by magnetic fields applied at any angle relative to the 2D plane (Kravchenko *et al* 1998) independently of the relative directions of the measuring current and magnetic field (Simonian *et al* 1997b; Pudalov *et al* 2002a). All these observations suggest that the giant magnetoresistance is due to coupling of the magnetic field to the electrons’ spins. Indeed, from an analysis of the positions of Shubnikov-de Haas oscillations in tilted magnetic fields, Okamoto *et al* (1999) and Vitkalov *et al* (2000, 2001a) have concluded that in MOSFETs at relatively high densities, the magnetic field B_{sat} is equal to that required to fully polarize the electrons’ spins.

In p -type GaAs/AlGaAs heterostructures, the effect of a parallel magnetic field is qualitatively similar, as shown in the right hand part of Fig. 13. The dependence

Metal-insulator transition in 2D

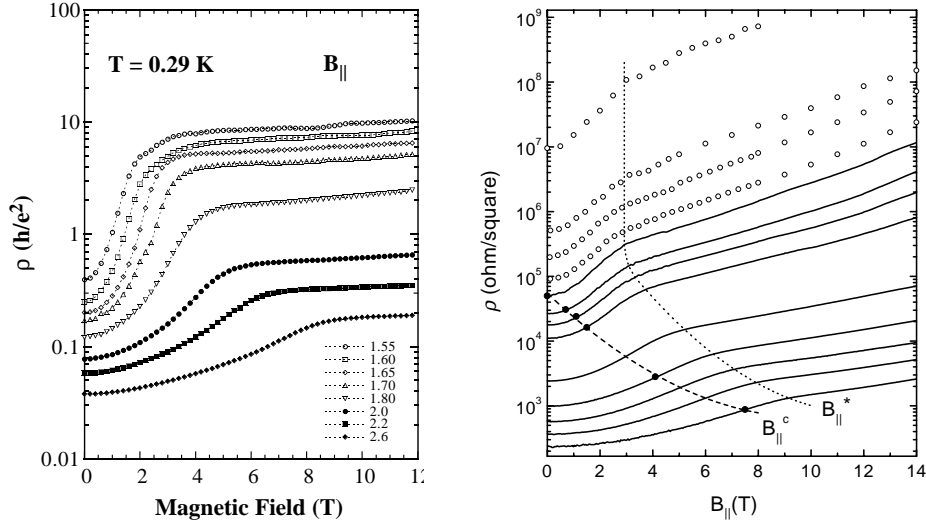


Figure 13. Left hand panel: resistivity versus parallel magnetic field measured at $T = 0.29$ K on low-disordered silicon sample. Different symbols correspond to densities from 1.01 to $2.17 \cdot 10^{11} \text{ cm}^{-2}$ (adopted from Pudalov *et al* 1997). Right hand panel: resistivity as a function of $B_{||}$ in a p-GaAs/AlGaAs heterostructure at 50 mK at the following hole densities, from the bottom: $4.11, 3.23, 2.67, 2.12, 1.63, 1.10, 0.98, 0.89, 0.83, 0.79, 0.75, 0.67 \cdot 10^{10} \text{ cm}^{-2}$. The solid lines are for hole densities above p_c and the open circles are for densities below p_c . The solid circles denote the experimentally determined critical magnetic fields, and the dashed line is a guide to the eye. $B_{||}^c$, the boundary separating the high and the low field regions, is shown by the dotted line. Adopted from Yoon *et al* (2000).

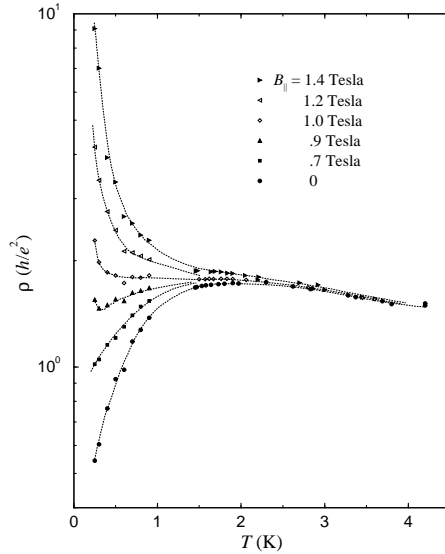


Figure 14. Resistivity versus temperature for five different fixed magnetic fields applied parallel to the plane of a low-disordered silicon MOSFET. The electron density is $8.83 \cdot 10^{10} \text{ cm}^{-2}$. From Simonian *et al* (1997b).

of ρ on B_{\parallel} does not saturate to a constant value as in Si MOSFETs, but continues to increase with increasing field, albeit at a considerably slower rate. This is presumably due to strong coupling of the parallel field to the orbital motion arising from the finite layer thickness (see Das Sarma and Hwang 2000), an effect that is more important in GaAs/AlGaAs heterostructures than in silicon MOSFETs because of a much thicker layer. As in the case of Si MOSFETs, there is a distinct knee that serves as a demarcation between the behaviour in low and high fields. For high hole densities, Shubnikov-de Haas measurements (Tutuc *et al* 2001) have shown that this knee is associated with full polarization of the spins by the in-plane magnetic field. However, unlike Si MOSFETs, the magnetoresistance in p-GaAs/AlGaAs heterostructures has been found to depend on the relative directions of the measuring current, magnetic field, and crystal orientation (Papadakis *et al* 2000); one should note that the crystal anisotropy of this material introduces added complications. In p-SiGe heterostructures, the parallel field was found to induce negligible magnetoresistance (Senz *et al* 1999) because in this system the parallel field cannot couple to the spins due to very strong spin-orbit interactions.

Over and above the very large magnetoresistance induced by an in-plane magnetic fields, an even more important effect of a parallel field is that it causes the zero-field 2D metal to become an insulator (Simonian *et al* 1997b; Mertes *et al* 2001; Shashkin *et al* 2001b; Gao *et al* 2002). Figure 14 shows how the temperature dependence of the resistance changes as the magnetic field is increased. Here, the resistivity of a Si MOSFET with fixed density on the metallic side of the transition is plotted as a function of temperature in several fixed parallel magnetic fields between 0 and 1.4 tesla. The zero-field curve exhibits behaviour typical for “just-metallic” electron densities: the resistivity is weakly-insulating at $T > T_{\max} \approx 2$ K and drops substantially as the temperature is decreased below T_{\max} . In a parallel magnetic field of only 1.4 tesla (the upper curve), the metallic drop of the resistivity is completely suppressed, so that the system is now strongly insulating in the entire temperature range. The effect of the field is negligible at temperatures above T_{\max} , *i.e.*, above the temperature below which the metallic behaviour in $B = 0$ sets in.

The extreme sensitivity to parallel field is also illustrated in Fig. 15 where the temperature dependence of the resistivity is compared in the absence (a) and in the presence (b) of a parallel magnetic field. For $B_{\parallel} = 0$, the resistivity displays the familiar, nearly symmetric (at temperatures above 0.2 K) critical behaviour about the separatrix (the dashed line). However, in a parallel magnetic field of $B_{\parallel} = 4$ tesla, which is high enough to cause full spin polarization at this electron density, all the $\rho(T)$ curves display “insulating-like” behaviour, including those which start below h/e^2 at high temperatures. There is no temperature-independent separatrix at any electron density in a spin-polarized electron system (Simonian *et al* 1997b; Shashkin *et al* 2001b).

This qualitative difference in behaviour demonstrates convincingly that the spin-polarized and unpolarized states behave very differently. This rules out explanations which predict qualitatively similar behaviour of the resistance regardless of the degree of spin polarization. In particular, the explanation of the metallic behaviour suggested by Das Sarma and Hwang (1999) (see also Lilly *et al* 2003), based on the temperature-dependent screening, predicts metallic-like $\rho(T)$ for both spin-polarized and unpolarized states, which is in disagreement with experiment (for more on this discrepancy, see Mertes *et al* 2001).

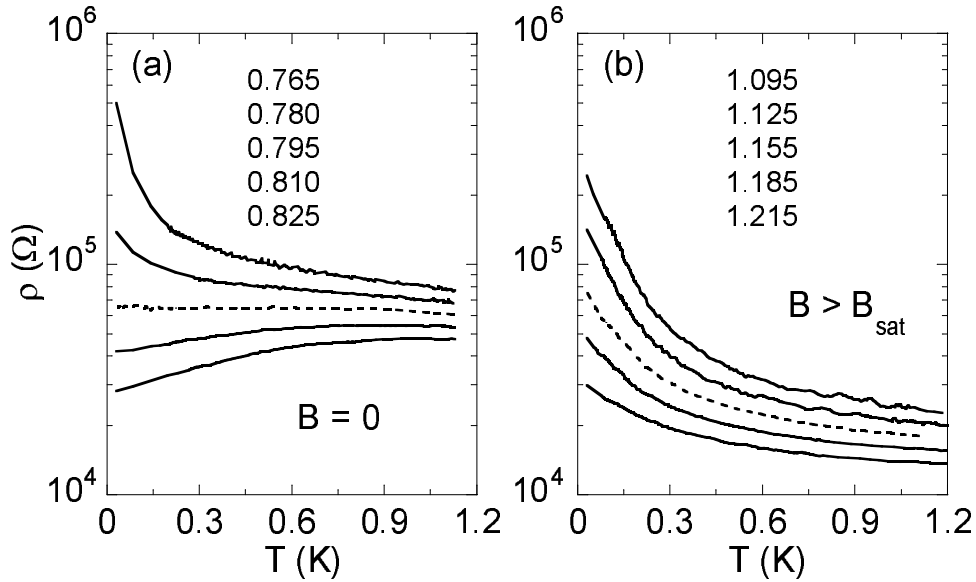


Figure 15. Temperature dependence of the resistivity of a low-disordered silicon MOSFET at different electron densities near the MIT in zero magnetic field (a), and in a parallel magnetic field of 4 tesla (b). The electron densities are indicated in units of 10^{11} cm^{-2} . Dashed curves correspond to $n_s = n_{c1}$ which is equal to $0.795 \cdot 10^{11} \text{ cm}^{-2}$ in zero field and to $1.155 \cdot 10^{11} \text{ cm}^{-2}$ in $B_{\parallel} = 4$ tesla. From Shashkin *et al* (2001b).

3.2. Scaling of the magnetoresistance; evidence for a phase transition

There have been many attempts to obtain a quantitative description of the magnetoresistance as a function of the carrier density and temperature over the entire field range, including the saturation region. Attempts to obtain a collapse of the magnetoresistance onto a single scaled curve have yielded scaling at either low or high magnetic field; over a wide range of temperatures but only at the metal-insulator transition; or in a wide range of carrier densities, but only in the limit of very low temperatures. Simonian *et al* (1998) found that at the transition, the deviation of the magnetoconductivity from its zero-field value, $\Delta\sigma \equiv \sigma(B_{\parallel}) - \sigma(0)$, is a universal function of B_{\parallel}/T . Although the quality of the scaling is good, it breaks down rather quickly as one moves into the metallic phase.

Two scaling procedures have been recently proposed; although they differ in procedure and yield results that differ somewhat in detail, the major conclusions are essentially the same, as described below, and imply that there is an approach to a quantum phase transition at a density near n_c .

Shashkin *et al* (2001a) scaled the magnetoresistivity in the spirit of the theory of Dolgoplov and Gold (2000), who predicted that at $T = 0$, the normalized magnetoresistance is a universal function of the degree of spin polarization, $P \equiv g^* \mu_B B_{\parallel} / 2E_F = g^* m^* \mu_B B_{\parallel} / \pi \hbar^2 n_s$ (here m^* is the effective mass and g^* is the g-factor). Shashkin *et al* scaled the data obtained in the limit of very low temperatures where the magnetoresistance becomes temperature-independent and, therefore, can be considered to be at its $T = 0$ value. In this regime, the normalized magnetoresistance,

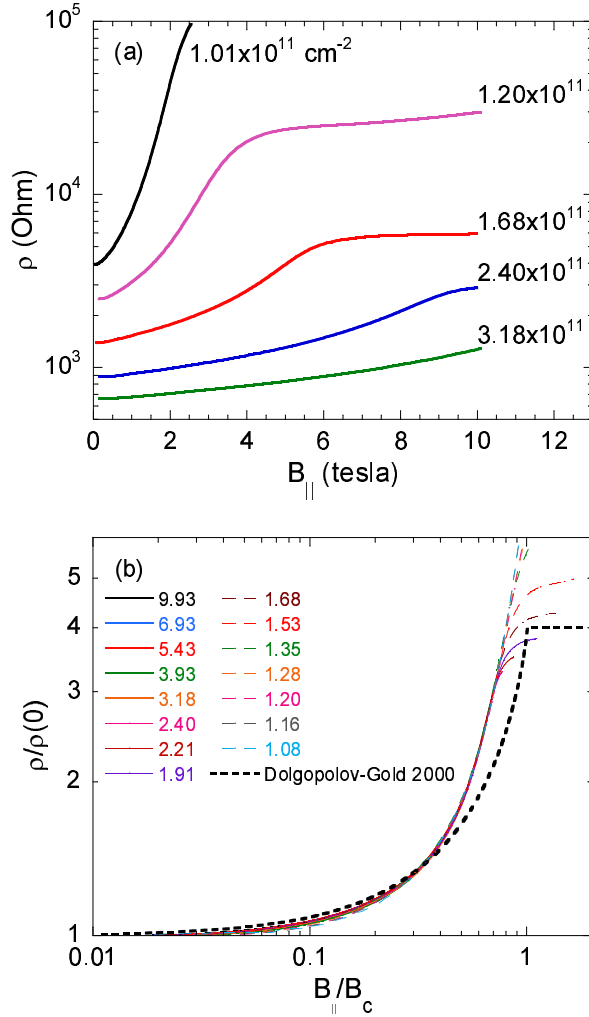


Figure 16. (a) Low-temperature magnetoresistance of a clean silicon MOSFET in parallel magnetic field at different electron densities above n_c . (b) Scaled curves of the normalized magnetoresistance versus $B_{||}/B_c$. The electron densities are indicated in units of 10^{11} cm^{-2} . Also shown by a thick dashed line is the normalized magnetoresistance calculated by Dolgoplov and Gold (2000). Adopted from Shashkin *et al* (2001a).

$\rho(B_{||})/\rho(0)$, measured at different electron densities, collapses onto a single curve when plotted as a function of $B_{||}/B_c$ (here B_c is the scaling parameter, normalized to correspond to the magnetic field B_{sat} at which the magnetoresistance saturates). An example of how $\rho(B_{||})$, plotted in Fig. 16 (a), can be scaled onto a universal curve is shown in Fig. 16 (b). The resulting function is described reasonably well by the theoretical dependence predicted by Dolgoplov and Gold. The quality of the scaling is remarkably good for $B_{||}/B_c \leq 0.7$ in the electron density range $1.08 \cdot 10^{11}$ to $10 \cdot 10^{11} \text{ cm}^{-2}$, but it breaks down as one approaches the metal-insulator transition where the magnetoresistance becomes strongly temperature-dependent even at the

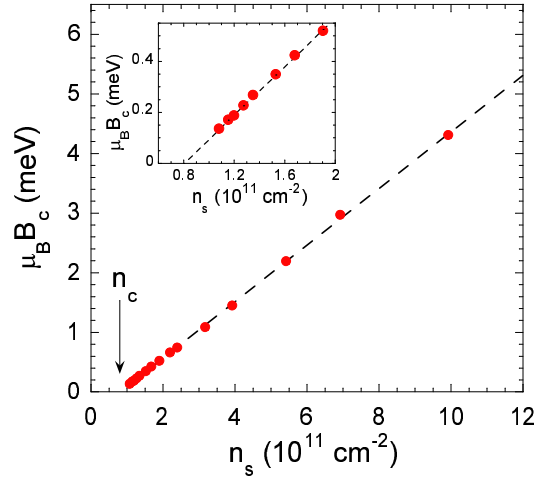


Figure 17. Scaling parameter B_c (corresponding to the field required for full spin polarization) as a function of the electron density. An expanded view of the region near n_c is displayed in the inset. From Shashkin *et al* (2001a).

lowest experimentally achievable temperatures. As shown in Fig. 17, the scaling parameter is proportional over a wide range of electron densities to the deviation of the electron density from its critical value: $B_c \propto (n_s - n_c)$.

Vitkalov *et al* (2001b) succeeded in obtaining an excellent collapse of magnetoconductivity data over a broad range of electron densities *and temperatures* using a single scaling parameter. They separated the conductivity into a field-dependent contribution, $\sigma(B_{\parallel}) - \sigma(\infty)$, and a contribution that is independent of magnetic field, $\sigma(\infty)$. The field-dependent contribution to the conductivity, $\sigma(0) - \sigma(B_{\parallel})$, normalized to its full value, $\sigma(0) - \sigma(\infty)$, was shown to be a universal function of B/B_{σ} :

$$\frac{\sigma(0) - \sigma(B_{\parallel})}{\sigma(0) - \sigma(\infty)} = F(B_{\parallel}/B_{\sigma}) \quad (2)$$

where $B_{\sigma}(n_s, T)$ is the scaling parameter. Applied to the magnetoconductance curves shown in Fig. 18 (a) for different electron densities, the above scaling procedure yields the data collapse shown in Fig. 18 (b).

Remarkably, similar scaling holds for curves obtained at different temperatures. This is demonstrated in Fig. 19, which shows the scaled magnetoconductance measured at a fixed density and different temperatures. Altogether, the scaling holds for temperatures up to 1.6 K over a broad range of electron densities up to $4n_c$.

Fig. 20 shows the scaling parameter B_{σ} plotted as a function of temperature for different electron densities $n_s > n_c$. The scaling parameter becomes smaller as the electron density is reduced; for a given density, B_{σ} decreases as the temperature decreases and approaches a value that is independent of temperature, $B_{\sigma}(T = 0)$. As the density is reduced toward n_c , the temperature dependence of B_{σ} dominates over a broader range and becomes stronger, and the low-temperature asymptotic value becomes smaller. Note that for electron densities below $1.36 \cdot 10^{11} \text{ cm}^{-2}$, B_{σ} is approximately linear with temperature at high T . The behaviour of the scaling

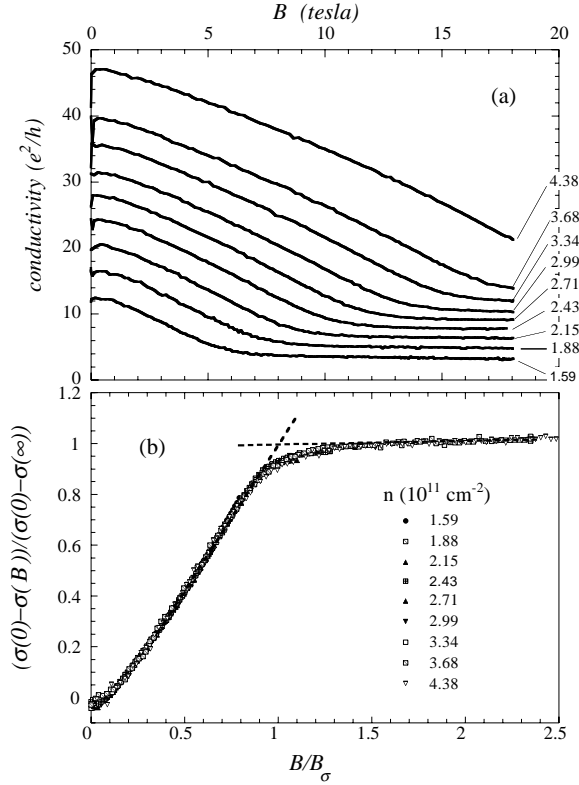


Figure 18. (a) Conductivity of a low-disordered silicon sample versus in-plane magnetic field at different electron densities in units of 10^{11} cm^{-2} , as labelled; $T = 100 \text{ mK}$. (b) Data collapse obtained by applying the scaling procedure, Eq.2, to the curves shown in (a). Adopted from Vitkalov *et al* (2001b).

parameter $B_\sigma(T)$ can be approximated by an empirical fitting function:

$$B_\sigma(n_s, T) = A(n_s)[\Delta(n_s)^2 + T^2]^{1/2}.$$

The solid lines in Fig. 20 (a) are fits to this expression using $A(n_s)$ and $\Delta(n_s)$ as fitting parameters. As can be inferred from the slopes of the curves of Fig. 20 (a), the parameter $A(n_s)$ is constant over most of the range and then exhibits a small increase (less than 20%) at lower densities. As shown in Fig. 20 (b), the parameter Δ decreases sharply with decreasing density and extrapolates to zero at a density n_0 which is within 10% of the critical density $n_c \approx 0.85 \cdot 10^{11} \text{ cm}^{-2}$ for the metal-insulator transition.

The scaling parameters B_c and Δ in the analysis by Shashkin *et al* (2001a) and Vitkalov *et al* (2001b) represent energy scales $\mu_B B_c$ and $k_B \Delta$, respectively, which vanish at or near the critical electron density for the metal-insulator transition. At high electron densities and low temperatures $T < \mu_B B_c / k_B$ (corresponding to $T < \Delta$), the system is in the zero temperature limit. As one approaches n_c , progressively lower temperatures are required to reach the zero temperature limit. At $n_s = n_0$, the energies $\mu_B B_c$ and $k_B \Delta$ vanish; the parameter $B_\sigma \rightarrow 0$ as $T \rightarrow 0$; the system thus

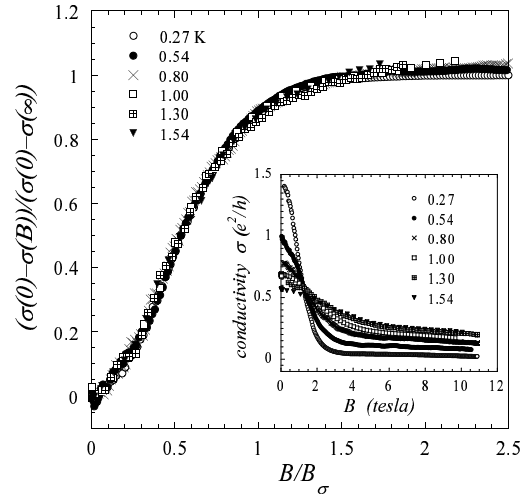


Figure 19. Data collapse obtained by applying the scaling procedure, Eq.2, to the magnetoconductivity at different temperatures for electron density $n_s = 9.4 \cdot 10^{10} \text{ cm}^{-2}$. The inset shows the conductivity at different temperatures as a function of magnetic field. Adopted from Vitkalov *et al* (2001b).

exhibits critical behaviour (Sondhi *et al* 1997; Vojta 2003), signalling the approach to a new phase in the limit $T = 0$ at a critical density $n_0 \approx n_c$.

4. SPIN SUSCEPTIBILITY NEAR THE METAL-INSULATOR TRANSITION

4.1. Experimental measurements of the spin susceptibility

In the Fermi-liquid theory, the electron effective mass and the g -factor (and, therefore, the spin susceptibility $\chi \propto g^* m^*$) are renormalized due to electron-electron interactions (Landau 1957). Earlier experiments (Fang and Stiles 1968; Smith and Stiles 1972), performed at relatively small values of $r_s \sim 2$ to 5, confirmed the expected increase of the spin susceptibility. More recently, Okamoto *et al* (1999) observed a renormalization of χ by a factor of ~ 2.5 at r_s up to about 6 (see Fig. 24 (a)). At yet lower electron densities, in the vicinity of the metal-insulator transition, Kravchenko *et al* (2000b) have observed a disappearance of the energy gaps at ‘‘cyclotron’’ filling factors which they interpreted as evidence for an increase of the spin susceptibility by a factor of at least 5.

It was noted many years ago by Stoner that strong interactions can drive an electron system toward a ferromagnetic instability (Stoner 1946). Within some theories of strongly interacting 2D systems (Finkelstein 1983, 1984; Castellani *et al* 1984), a tendency towards ferromagnetism is expected to accompany metallic behaviour. The experiments discussed in Section 3.2 which indicate that B_c and Δ vanish at a finite density prompted Shashkin *et al* (2001a) and Vitkalov *et al* (2001b) to suggest that spontaneous spin polarization may indeed occur at or near the critical electron density in the limit $T = 0$. The data obtained in these experiments provide information from which the spin susceptibility, χ , can be calculated in a wide range of

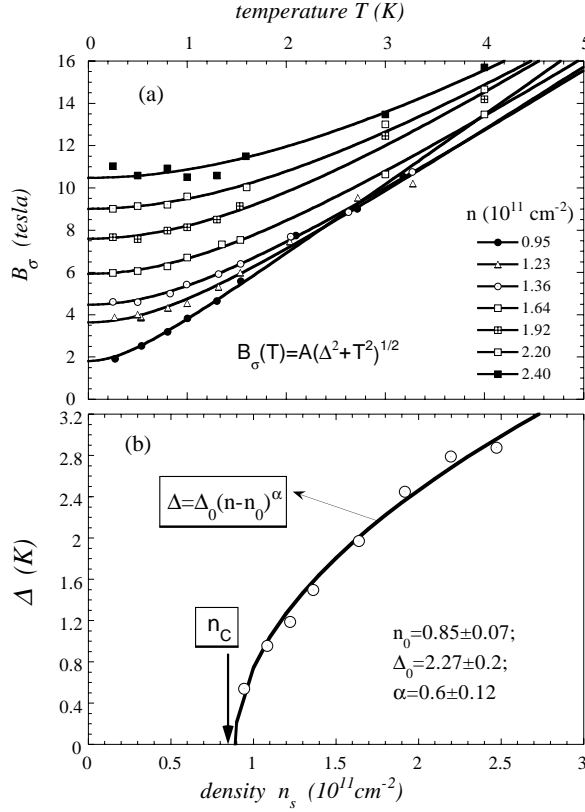


Figure 20. (a) B_σ versus temperature for different electron densities; the solid lines are fits to the empirical form $B_\sigma(n_s, T) = A(n_s)[\Delta(n_s)]^2 + T^2]^{1/2}$. (b) The parameter Δ as a function of electron density; the solid line is a fit to the critical form $\Delta = \Delta_0(n_s - n_0)^\alpha$. From Vitkalov *et al* (2001b).

densities. In the clean limit, the band tails are small (Vitkalov *et al* 2002; Dolgoplov and Gold 2002; Gold and Dolgoplov 2002) and can be neglected, and the magnetic field required to fully polarize the spins is related to the g -factor and the effective mass by the equation $g^* \mu_B B_c = 2E_F = \pi \hbar^2 n_s / m^*$ (here, the two-fold valley degeneracy in silicon has been taken into account). Therefore, the spin susceptibility, normalized by its “non-interacting” value, can be calculated as

$$\frac{\chi}{\chi_0} = \frac{g^* m^*}{g_0 m_b} = \frac{\pi \hbar^2 n_s}{2 \mu_B B_c m_b}.$$

Fig. 21 shows the normalized spin susceptibility (Shashkin *et al* 2001a) and its inverse (Vitkalov *et al* 2002) obtained using the above expression. The values deduced by both groups indicate that $g^* m^*$ diverges ($(g^* m^*)^{-1}$ extrapolates to zero) in silicon MOSFETs at a finite density close or equal to n_c . Also shown on the same figure are the data of Pudalov *et al* obtained from an analysis of Shubnikov-de Haas (SdH) measurements in crossed magnetic fields (see section 4.2). The susceptibilities obtained by all three groups on different samples, by different methods and in different ranges of magnetic field, are remarkably similar (on the mutual consistency of the data obtained

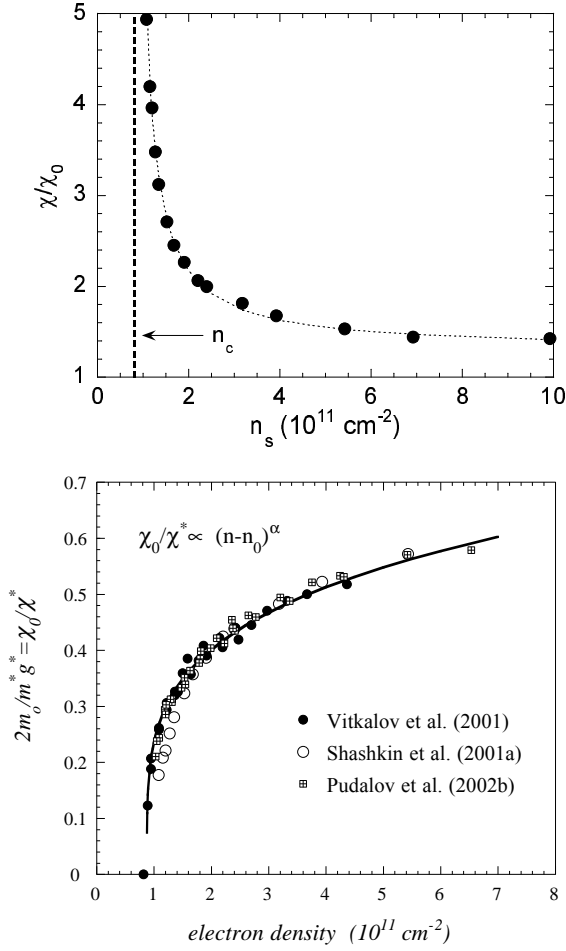


Figure 21. Upper graph: normalized spin susceptibility *vs* n_s obtained from the data in Fig. 17. The dashed line is a guide to the eye. The vertical dashed line denotes the position of the critical density for the metal-insulator transition. Lower graph: the inverse of the normalized spin susceptibility χ_0/χ^* versus electron density obtained by Vitkalov *et al* (2001b), plotted with data of Shashkin *et al* (2001a) and Pudalov *et al* (2002b). The solid curve is a fit to the critical form $\chi_0/\chi^* = A(n_s - n_0)^\alpha$ for the data of Vitkalov *et al* (2001b) (excluding the point shown at $\chi_0/\chi^* = 0$). Adopted from Vitkalov *et al* (2002).

on different samples by different groups, see also Kravchenko *et al* (2002) and Sarachik and Vitkalov (2003)).

A novel and very promising method has recently been used by Prus *et al* (2003) to obtain direct measurements of the thermodynamic spin susceptibility. The method entails modulating the (parallel) magnetic field by an auxiliary coil and measuring the AC current induced between the gate and the 2D electron gas, which is proportional to $\partial\mu/\partial B$ (where μ is the chemical potential). Using Maxwell's relation,

$$\frac{\partial\mu}{\partial B} = -\frac{\partial M}{\partial n_s},$$

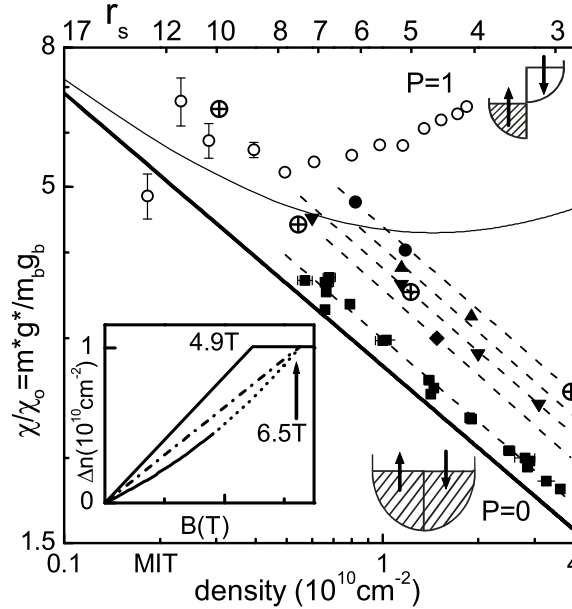


Figure 22. Density-dependence of m^*g^* in an ultra-clean 2D electron system in GaAs/AlGaAs determined by two different methods. The solid data points are obtained from tilted-field Shubnikov-de Haas measurements with different configurations of Landau levels. The parallel dashed lines indicate a power law dependence of m^*g^* with a single exponent for all level configurations. The open circles show nonmonotonic density-dependence of m^*g^* derived from the full polarization field, B_c , using the parallel field method. The inset shows the net spin for $n_s = 1 \cdot 10^{10} \text{ cm}^{-2}$ with interpolated regime (solid line) and extrapolated regime (dotted line). $B_c=4.9\text{T}$ from the in-plane field method and $B_{ext}=6.5 \text{ T}$ from extrapolation of the tilted-field method. The thick solid line represents extrapolation of m^*g^* to the $P=0$ limit. Calculations from Attacalite *et al* (2002) are shown as crossed circles. Adopted from Zhu *et al* (2003).

one can obtain the magnetization M by integrating the induced current over n_s . The magnetic susceptibility can then be determined from the slope of the $M(B)$ versus B dependence at small fields. To date, Prus *et al* have reported data for one sample which becomes insulating at a relatively high electron density ($1.3 \cdot 10^{11} \text{ cm}^{-2}$), and the data obtained below this density are irrelevant for the metallic regime we are interested in. For this reason, the data collected so far do not provide information about the most interesting regime just above n_χ .

In GaAs/AlGaAs heterostructures, a similar strong increase of the spin susceptibility at ultra-low carrier densities has now been established based on an analysis of the Shubnikov-de Haas oscillations (Zhu *et al* 2003). The results are shown in Fig. 22 by solid symbols; χ increases by more than a factor of two as the density decreases. Zhu *et al* suggested an empirical equation $\chi \propto n_s^{-0.4}$ to describe their experimental data, which works well in the entire range of electron densities spanned. Although χ tends toward a divergence, it is not clear from these experiments whether it does so at a finite density. We note that due to the lower effective mass, higher dielectric constant and the absence of valley degeneracy, the ratio r^* between Coulomb and Fermi energies in GaAs/AlGaAs is an order of magnitude smaller than

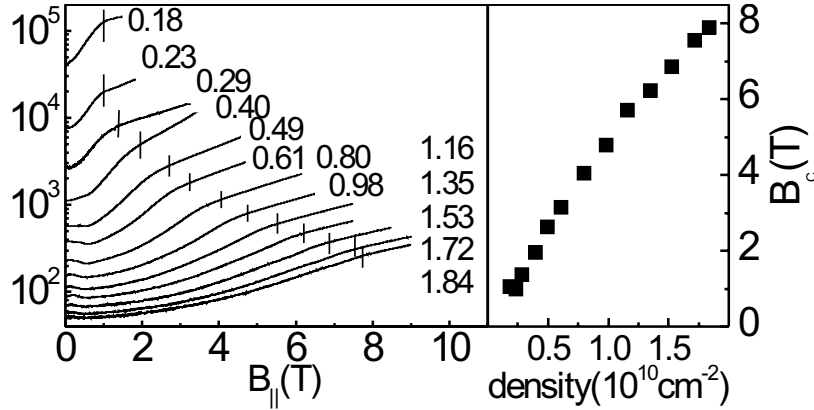


Figure 23. Left hand panel: magnetoconductance of GaAs/AlGaAs as a function of in parallel-field for different electron densities indicated in unit of 10^{10} cm^{-2} ; the positions of the magnetic fields, B_c , required for full polarization are indicated following Tutuc *et al* (2002). Right hand panel: B_c as a function of density. Adopted from Zhu *et al* (2003).

in silicon MOSFETs at the same electron density; therefore, to reach the same relative interaction strength, samples are required which remain metallic at densities about two orders of magnitude lower than in silicon, *i.e.*, $< 10^9 \text{ cm}^{-2}$. The currently accessible electron densities in GaAs/AlGaAs heterostructures are still too high to reliably establish the limiting behaviour of χ .

The open circles in Fig. 22 denote $\chi(n_s)$ derived from an alternative method for measuring B_c based on a determination of the parallel magnetic field corresponding to the “knee” of the magnetoconductance curves, as shown in the left hand panel of Fig. 23. Earlier, this method yielded an anomalous and quite puzzling decrease of the susceptibility with decreasing density in both hole (Tutuc *et al* 2002) and electron (Noh *et al* 2002) systems in GaAs/AlGaAs. This was in disagreement with findings in Si MOSFETs, and argued against any spontaneous spin polarization. These results are now believed to be in error for a number of possible reasons. The field for full spin polarization, marked by vertical bars in Fig. 23 (left hand panel) and plotted as a function of n_s in Fig. 23 (right hand panel), decreases with decreasing carrier density and exhibits an apparent saturation below $n_s \approx 0.23 \cdot 10^{10} \text{ cm}^{-2}$. Calculation based on this saturation field would yield a spin susceptibility that decreases below this density. However, the saturation field may be constant below this density due to the fact that the experiments are performed at a temperature which is too high; if the temperature were decreased further, the saturation field would probably continue to decrease, consistent with the decrease of B_σ shown in Fig. 20 (a). Another possible source of error is the finite thickness of the electron layer in GaAs/AlGaAs heterostructures, which leads to an increase in the effective mass with increasing parallel magnetic field (Batke and Tu 1986). Indeed, it has recently been shown by Zhu *et al* (2003) that the conclusion that the spin susceptibility decreases with decreasing carrier density is erroneous and originates from the fact that the effective mass depends on magnetic field. The effect of the finite thickness on the spin susceptibility was studied in detail by Tutuc *et al* (2003).

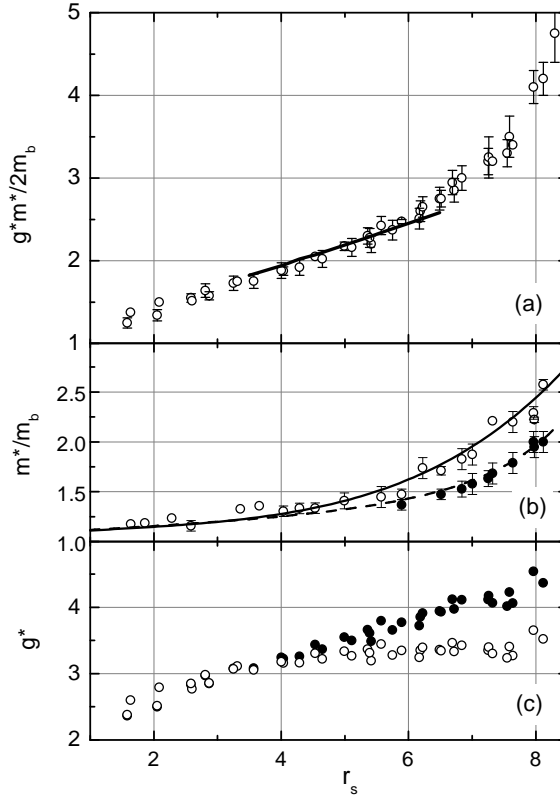


Figure 24. The parameters g^*m^* , m^* , and g^* for different silicon samples as a function of r_s (dots). The solid line in (a) shows the data of Okamoto *et al* (1999). The solid and open dots (b) and (c) correspond to two different methods of finding m^* (see the text). The solid and dashed lines in (b) are polynomial fits for the two functions for $m^*(r_s)$. Adopted from Pudalov *et al* (2002).

4.2. Effective mass and g-factor

In principle, the increase of the spin susceptibility could be due to an enhancement of either g^* or m^* (or both). To obtain g^* and m^* separately, Pudalov *et al* (2002b) performed measurements of SdH oscillations in superimposed and independently controlled parallel and perpendicular magnetic fields. Their results are shown in Fig. 24. The data were taken at relatively high temperatures (above 300 mK), where the low- n_s resistance depends strongly on temperature. Therefore, the conventional procedure of calculating the effective mass from the temperature dependence of the amplitude of the SdH oscillations is unreliable, as it assumes a temperature-independent Dingle temperature. Pudalov *et al* considered two limiting cases: a temperature-independent T_D , and a T_D that linearly increases with temperature; two sets of data based on these assumptions are plotted in Fig. 24 (b) and (c). Within the uncertainty associated with the use of these two methods, both g^* and m^* were found to increase with decreasing n_s .

Shashkin *et al* (2002) used an alternative method to obtain g^* and m^* separately. They analyzed the data for the temperature dependence of the conductivity in zero magnetic field using the recent theory of Zala *et al* (2001). According to this theory,

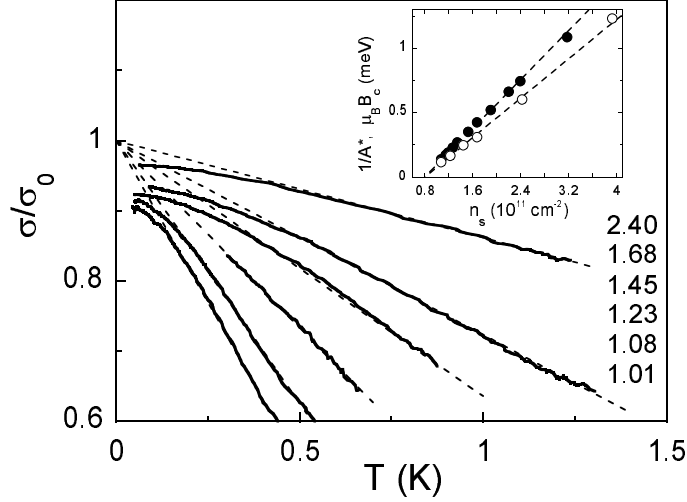


Figure 25. For a low-disordered silicon MOSFET, the temperature dependence of the normalized conductivity at different electron densities (indicated in units of 10^{11} cm^{-2}) above the critical electron density for the metal-insulator transition. The dashed lines are fits to the linear portions of the curves. The inset shows $1/A^*(n_s)$ (see Eq. 3) and $B_c(n_s)$ (open and solid circles, respectively). The dashed lines are continuations of the linear fits, which extrapolate to the critical electron density for the metal-insulator transition. From Shashkin *et al* (2002).

σ is a linear function of temperature:

$$\frac{\sigma(T)}{\sigma_0} = 1 - A^* k_B T, \quad (3)$$

where the slope, A^* , is determined by the interaction-related parameters: the Fermi liquid constants F_0^a and F_1^s :

$$A^* = -\frac{(1 + 8F_0^a)g^*m^*}{\pi\hbar^2 n_s}, \quad \frac{g^*}{g_0} = \frac{1}{1 + F_0^a}, \quad \frac{m^*}{m_b} = 1 + F_1^s \quad (4)$$

(here $g_0 = 2$ is the “bare” g -factor.) These relations allow a determination of the many-body enhanced g^* factor and mass m^* separately using the data for the slope A^* and the product g^*m^* .

The dependence of the normalized conductivity on temperature, $\sigma(T)/\sigma_0$, is displayed in Fig. 25 at different electron densities above n_c ; the value of σ_0 used to normalize σ was obtained by extrapolating the linear interval of the $\sigma(T)$ curve to $T = 0$. The inverse slope $1/A^*$ (open circles) and $B_c(n_s)$ (solid circles) are plotted as a function of n_s in the inset to Fig. 25. Over a wide range of electron densities, $1/A^*$ and $\mu_B B_c$ are close to each other; the low-density data for $1/A^*$ are approximated well by a linear dependence which extrapolates to the critical electron density n_c in a way similar to B_c .

Values of g^*/g_0 and m^*/m_b determined from this analysis are shown as a function of the electron density in Fig. 26. In the high n_s region (relatively weak interactions), the enhancement of both g and m is relatively small, both values increasing slightly with decreasing electron density in agreement with earlier data (Ando *et al* 1982). Also, the renormalization of the g -factor is dominant compared to that of the effective

mass, consistent with theoretical studies (Iwamoto 1991; Kwon *et al* 1994; Chen and Raikh 1999). In contrast, the renormalization at low n_s (near the critical region), where $r_s \gg 1$, is much more striking. As the electron density is decreased, the

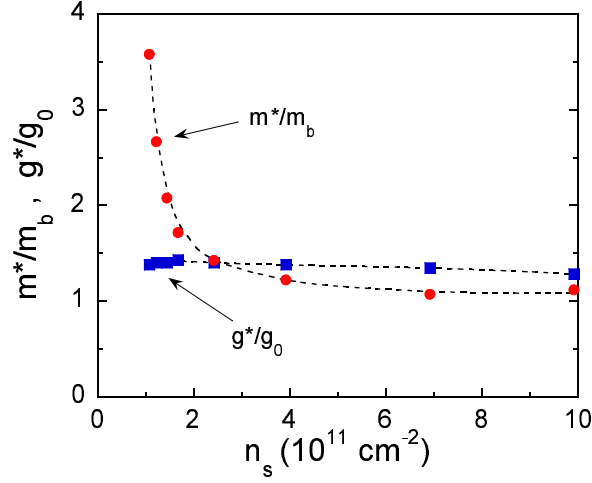


Figure 26. The effective mass (circles) and g factor (squares) in a silicon MOSFET, determined from the analysis of the parallel field magnetoresistance and temperature-dependent conductivity, versus electron density. The dashed lines are guides to the eye. From Shashkin *et al* (2002).

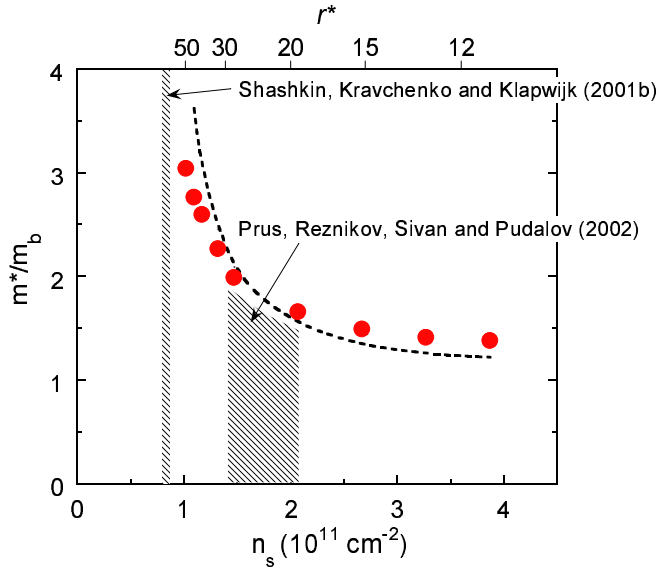


Figure 27. For a silicon MOSFET, the effective mass obtained from an analysis of $\rho(B_{\parallel})$ (dotted line) and from an analysis of SdH oscillations (circles). Data of Shashkin *et al* (2003a). The upper x-axis shows r^* calculated using the latter value for the effective mass. The shaded areas correspond to metallic regimes studied in papers by Shashkin *et al* (2001b) and Prus *et al* (2002), as labelled.

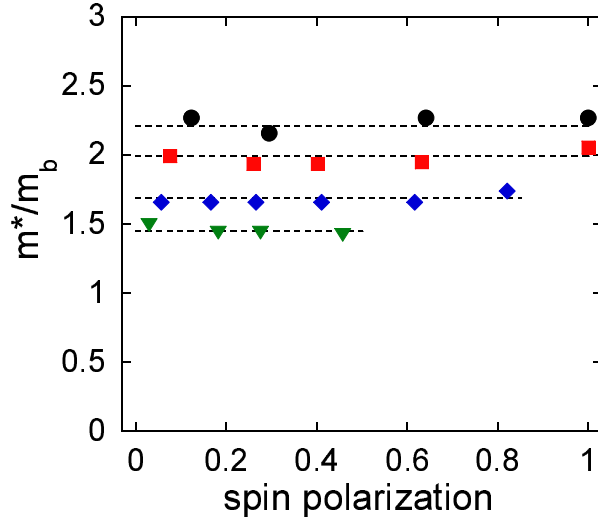


Figure 28. For silicon MOSFETs, the effective mass versus the degree of spin polarization for the following electron densities in units of 10^{11} cm $^{-2}$: 1.32 (dots), 1.47 (squares), 2.07 (diamonds), and 2.67 (triangles). The dashed lines are guides to the eye. From Shashkin *et al* (2003a).

renormalization of the effective mass increases markedly with decreasing density while the g factor remains relatively constant. Hence, this analysis indicates that it is the effective mass, rather than the g -factor, that is responsible for the strongly enhanced spin susceptibility near the metal-insulator transition. To verify this conclusion, Shashkin *et al* (2003a, 2003b) used an independent method to determine the effective mass through an analysis of the temperature dependence of the SdH oscillations similar to the analysis done by Smith and Stiles (1972) and Pudalov *et al* (2002b), but extended to much lower temperatures where the Dingle temperature is expected to be constant and the analysis reliable. In Fig. 27, the effective mass obtained by this method is compared with the results obtained by the procedure described above (the dotted line). The quantitative agreement between the results obtained by two independent methods supports the validity of both. The data for the effective mass are also consistent with data for spin and cyclotron gaps obtained by magnetocapacitance spectroscopy (Khrapai *et al* 2003).

To probe a possible connection between the effective mass enhancement and spin and exchange effects, Shashkin *et al* (2003a, 2003b) introduced a parallel magnetic field component to align the electrons' spins. In Fig. 28, the effective mass is shown as a function of the spin polarization, $P = (B_{\perp}^2 + B_{\parallel}^2)^{1/2}/B_c$. Within the experimental accuracy, the effective mass does not depend on P . Therefore, the enhancement of m^* near the MIT is robust, and the origin of the mass enhancement has no relation to the electrons' spins and exchange effects.

4.3. Electron-electron interactions near the transition

The interaction parameter, $r^* \equiv E_C/E_F$, is generally assumed to be equal to the dimensionless Wigner-Seitz radius, $r_s = 1/(\pi n_s)^{1/2} a_B$, and, hence, proportional to

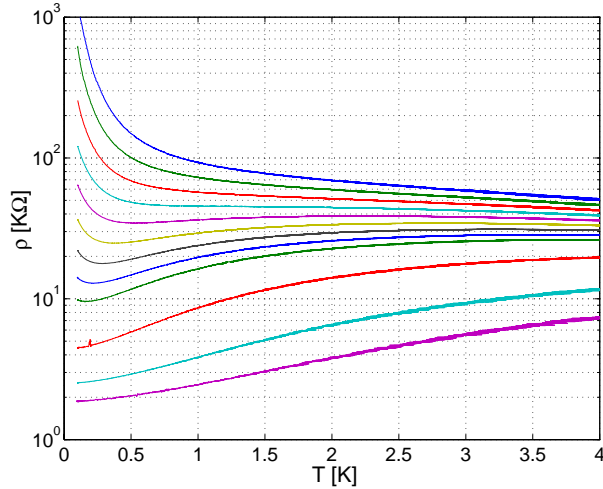


Figure 29. $\rho(T)$ in a moderately disordered silicon MOSFET. Densities from top to bottom are $n_s = 1.20$ to 1.44 (in 0.03 steps), 1.56 , 1.8 and $2.04 \cdot 10^{11} \text{ cm}^{-2}$. From Prus *et al* (2002).

$n_s^{-1/2}$. However, this is true only if the effective mass does not depend on n_s ; close to the transition, where the effective mass is strongly enhanced, the deviations from the square root law become important, and the interaction parameter is larger than the Wigner-Seitz radius by a factor of m^*/m_b (or $2m^*/m_b$ in silicon MOSFETs, where an additional factor of 2 derives from the valley degeneracy).

Near the metal-insulator transition, r^* grows rapidly due to the sharp increase of the effective mass, as shown on the upper x -axis in figure 27; here r^* is calculated using the effective mass obtained from the analysis of the SdH oscillations. We note that since at low n_s this method yields a somewhat smaller effective mass than the method based on the analysis of $\rho(B_{\parallel})$, the plotted values represent the most conservative estimate for r^* . Due to the rapid increase of m^* near the transition, even small changes in the electron density may lead to large changes in r^* . For example, the transition to a localized state in a low-disordered sample used by Shashkin *et al* (2001b) occurs at $n_s = 0.795 \cdot 10^{11} \text{ cm}^{-2}$ (see Fig. 15), while in a sample of lesser quality used by Prus *et al* (2002), it occurs at $1.44 \cdot 10^{11} \text{ cm}^{-2}$ (see Fig. 29). The areas corresponding to the metallic regimes studied in these papers are shaded in Fig. 27; the corresponding values of r^* differ dramatically (the actual values of r^* in the study by Shashkin *et al* are not known because the effective mass has not been determined near the transition; the lower boundary for r^* is 50). The difference in r^* may account for the qualitative change in the behaviour of the resistance in the two samples: in the more disordered sample, there is no temperature-independent curve (the separatrix), and some of the curves which look “metallic” at higher temperature are insulating below a few hundred mK, suggesting that localization becomes dominant in this sample as $T \rightarrow 0$.

5. HOW DOES ALL THIS FIT THEORY?

The possibility that a $B = 0$ metallic state in 2D can be stabilized by interactions was first suggested by Finkelstein (1983, 1984) and Castellani *et al* (1984). In this

theory, the combined effects of disorder and interactions were studied by perturbative renormalization group methods. It was found that as the temperature is decreased, the resistivity increases and then decreases at lower temperatures, suggesting that the system is approaching a low-temperature metallic state. An external magnetic field, via Zeeman splitting, drives the system back to the insulating state. These predictions of the theory are in qualitative agreement with experiments.

However, an interaction parameter scales to infinitely large values before zero temperature is reached, and the theory thus becomes uncontrolled; this scenario has consequently not received general acceptance. It should also be noted that the theory may not be applicable to the current experiments since it was developed for the diffusive regime: $T \ll \hbar/\tau$, where τ is the elastic mean-free time extracted from the Drude conductivity (Boltzmann constant is assumed to be equal to 1 throughout this section). This condition corresponds to the low-temperature limit $T \ll T_F \rho / (h/e^2)$. Since the Fermi temperature, T_F , is rather low at the small carrier densities considered here, the above condition is satisfied only close to the transition, where ρ becomes of the order of h/e^2 . In the experiments, however, the characteristic decrease of the resistance with decreasing temperature often persists into the relatively high-temperature *ballistic* regime $T > \hbar/\tau$ (or $T > T_F \rho / (h/e^2)$). Altshuler *et al* (2001) and Brunthaler *et al* (2001) have interpreted this observation as evidence that the mechanism responsible for the strong temperature dependence cannot originate from quantum interference.

For the ballistic region, calculations in the random phase approximation were carried out two decades ago by Stern (1980), Gold and Dolgoplov (1986), Das Sarma (1986) and were recently refined by Das Sarma and Hwang (1999). These theories predict a linear temperature dependence for the conductivity with metallic-like slope ($d\sigma/dT < 0$) regardless of the strength of the interactions. The spin degree of freedom is not important in this theory and enters only through the Fermi energy, which is a factor of two larger for the spin-polarized than for the unpolarized system. Therefore, the application of a (parallel) magnetic field does not eliminate the metallic temperature dependence.

The two limits — diffusive and ballistic — had until recently been assumed to be governed by different physical processes. However, Zala *et al* (2001) have shown that the temperature dependence of the conductivity in the ballistic regime originates from the same physical process as the Altshuler-Aronov-Lee corrections: coherent scattering of electrons by Friedel oscillations. In this regime the correction is linear in temperature, as is the case for the results mentioned in the previous paragraph. However, the value and even the *sign* of the slope depends on the strength of electron-electron interaction, the slope being directly related to the renormalization of the spin susceptibility (see also Gold 2001, 2003). By aligning the spins, a magnetic field causes a positive magnetoresistance and changes the temperature dependence of the conductivity from metallic-like to insulating-like (Herbut 2001; Zala *et al* 2002; Gold 2003), in agreement with experiments.

5.1. The diffusive regime: Renormalization group analysis

It is well known that in the diffusive limit ($T\tau \ll \hbar$), electron-electron interactions in two dimensional disordered systems lead to logarithmically divergent corrections to

the conductivity given by:

$$\delta\sigma = -\frac{e^2}{2\pi^2\hbar} \ln\left(\frac{\hbar}{T\tau}\right) \left[1 + 3\left(1 - \frac{\ln(1 + F_0^\sigma)}{F_0^\sigma}\right)\right], \quad (5)$$

where F_0^σ is the interaction constant in the triplet channel which depends on the interaction strength. The sign of this logarithmically divergent correction may be positive (metallic-like) or negative (insulating-like), depending on the value of F_0^σ .

Experimentally, the diffusive regime is realized in a relatively narrow range of electron densities near the metal-insulator transition, where the resistivity is of the order of h/e^2 . Punnoose and Finkelstein (2002) have convincingly demonstrated that in this region, the temperature dependence of the resistivity can be understood within the renormalization group theory describing the effect of the electron-electron interactions on the propagation of diffusive collective modes, with the *delocalizing* component becoming dominant in dilute 2D systems.

In 2D, the renormalization group equation describing the evolution of the resistivity has been derived previously by Finkelstein:

$$\frac{dg}{d\xi} = g^2 \left[1 + 1 - 3\left(\frac{1 + \gamma_2}{\gamma_2} \ln(1 + \gamma_2) - 1\right)\right]. \quad (6)$$

Here $\xi = -\ln(T\tau/\hbar)$, the dimensionless parameter g is the conductance in units of $e^2/\pi h$ and γ_2 is the coupling constant. The first term in the square brackets of Eq. 6 corresponds to the weak localization correction (quantum interference; Abrahams *et al* 1979), while the second term is the contribution of the singlet density mode which is due to the long range nature of the Coulomb interaction (Altshuler, Aronov and Lee 1980). The last term describes the contribution of the three triplet modes. Note that the last two terms have opposite signs, favouring localization and delocalization, respectively. The resulting dependence $g(\xi)$ becomes delocalizing when $\gamma_2 > \gamma_2^* = 2.04$. This requires the presence of rather strong electron correlations.

In the case of two distinct valleys (as in (100) silicon MOSFETs), Eq. 6 can be easily generalized to:

$$\frac{dg}{d\xi} = g^2 \left[2 + 1 - 15\left(\frac{1 + \gamma_2}{\gamma_2} \ln(1 + \gamma_2) - 1\right)\right]. \quad (7)$$

The difference between the numerical factors in Eq. 6 and Eq. 7 results from the number of degrees of freedom in each case. The weak localization term becomes twice as large. The difference in the number of the multiplet modes increases the coefficient of the γ_2 term from 3 to 15. As a result of these modifications, the value of γ_2 required for the dependence $g(\xi)$ to become delocalizing is reduced to $\gamma_2^* = 0.45$. which makes it easier in the case of two valleys to reach the condition where the resistivity decreases with decreasing temperature.

In conventional conductors the initial values of γ_2 are small, and the net effect is in favour of localization. In dilute systems, however, this value is enhanced due to electron-electron correlations. In addition, γ_2 also experiences logarithmic corrections due to the disorder (Finkelstein 1983, 1984; Castellani *et al* 1984, 1998). The equation describing the renormalization group evolution of γ_2 is the same for the case of one and two valleys:

$$\frac{d\gamma_2}{d\xi} = g \frac{(1 + \gamma_2)^2}{2}. \quad (8)$$

It follows from this equation that γ_2 increases monotonically as the temperature is decreased. Once it exceeds γ_2^* , the resistivity passes through a maximum. Even though

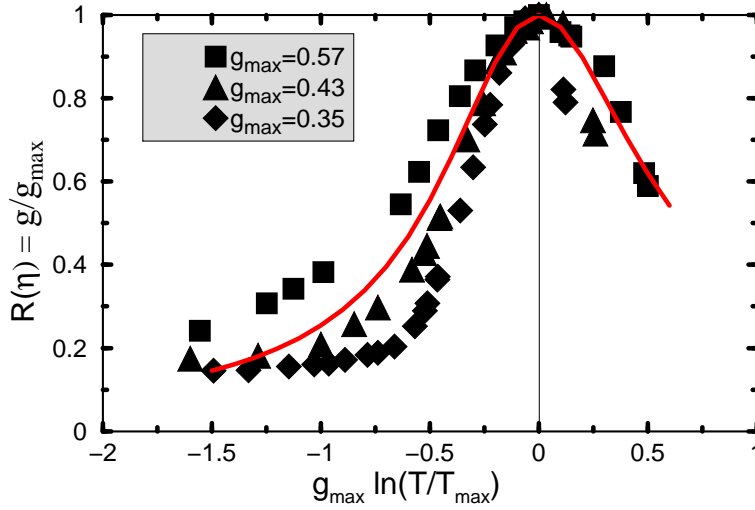


Figure 30. Data for silicon MOSFETs at $n_s = 0.83, 0.88$ and $0.94 \cdot 10^{11} \text{ cm}^{-2}$ from Pudalov *et al* (1998) are scaled according to Eq. 9. The solid line corresponds to the solution of the renormalization group, Eqs. 7 and 8; no adjustable parameters were used in this fit. From Punnoose and Finkelstein (2002).

the initial values of g and γ_2 are not universal, the flow of g can be described by a universal function $R(\eta)$ (Finkelstein, 1983):

$$g = g_{\max} R(\eta) \text{ and } \eta = g_{\max} \ln(T_{\max}/T), \quad (9)$$

where T_{\max} is the temperature at which g reaches its maximum value g_{\max} .

In Fig. 30, the theoretical calculations are compared with the experimental data obtained by Pudalov *et al* (1998). Since the renormalization group equations were derived in the lowest order in g and cannot be applied in the critical region where $g > 1$, only curves with maximum g ranging from $g_{\max} \approx 0.3$ to $g_{\max} \approx 0.6$ are shown in the figure. The decrease in the resistivity by up to a factor of five, as well as its saturation, are both captured in the correct temperature interval by this analysis without any adjustable parameters.

In agreement with experiment, this universal behaviour can be observed only in ultra clean samples (with negligible inter-valley scattering) and will not be found in samples that are only moderately clean. In disordered silicon MOSFETs, a description in terms of an effective *single* valley is relevant, and the large value of $\gamma_2^* = 2.04$ makes it difficult for the non-monotonic $\rho(T)$ to be observed as the initial values of γ_2 are usually much less than 2.04. As a result, for g near the critical region, the resistivity becomes insulating-like instead of going through the maximum.

Therefore, in ultra clean silicon MOSFETs, the behaviour of the resistivity not far from the transition is quantitatively well described by the renormalization group analysis that considers the interplay of the electron-electron interactions and disorder when the electron band has two distinct valleys. The theory in this case remains in control down to exponentially low temperatures, unlike the single valley case, where γ_2 diverges at $\eta \approx 1$, or at temperatures just below T_{\max} . A parallel magnetic field provides a Zeeman splitting and gives rise to positive magnetoresistance (Lee

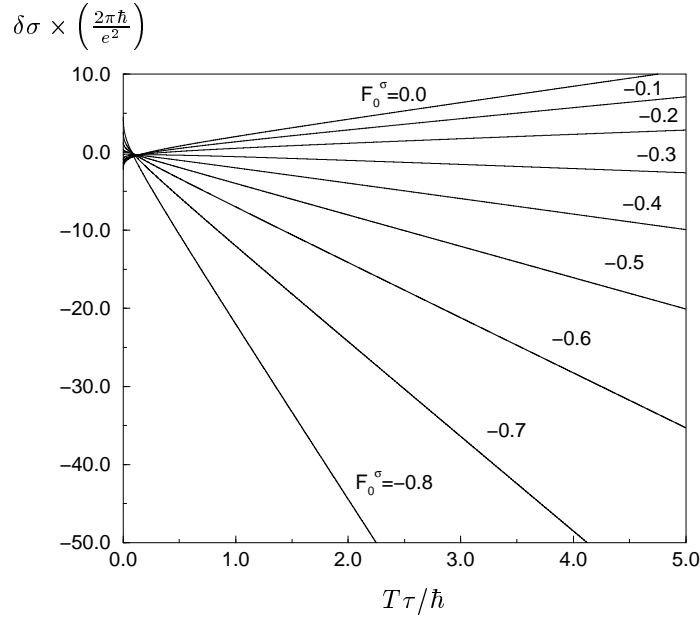


Figure 31. Total interaction correction to the conductivity. The curve for $F_0^\sigma = 0$ corresponds to the universal behaviour of a completely spin polarized electron gas. From Zala *et al* (2001).

and Ramakrishnan 1982; Finkelstein 1984; Castellani *et al* 1998). In a very strong magnetic field, when the electrons are completely spin-polarized, the system becomes “spinless”. In this case, the system always scales to an insulator, and in the weak disorder limit, a universal logarithmic temperature dependence is expected:

$$\sigma(T) = \sigma_0 + (e^2/\pi h)(2 - 2 \ln 2) \ln(T\tau/\hbar).$$

5.2. Farther from the transition (the ballistic regime)

Far from the transition ($n_s \gg n_c$), the inverse scattering time τ^{-1} is often smaller than the temperature at which the experiments are performed, and one is in the ballistic regime: $T\tau \gg \hbar$. The interaction theory by Zala *et al* (2001) considers coherent electron scattering off the Friedel oscillations. The phase of the Friedel oscillation is such that the wave scattered from the impurity interferes constructively with the wave scattered from the oscillation, leading to a quantum correction to the Drude conductivity, σ_0 . As has already been mentioned, this correction ($\Delta\sigma$), which is logarithmic in the diffusive regime, becomes linear in the ballistic regime:

$$\Delta\sigma(T) = \frac{e^2}{\pi\hbar} \frac{T\tau}{\hbar} \left(1 + \frac{3F_0^\sigma}{1 + F_0^\sigma}\right) = \sigma_0 \left(1 + \frac{3F_0^\sigma}{1 + F_0^\sigma}\right) \frac{T}{T_F} \quad (10)$$

where F_0^σ is the Fermi liquid interaction parameter in the triplet channel. As in the diffusive regime, the sign of $d\rho/dT$ depends on the constant F_0^σ .

The total correction to the conductivity is shown in Fig. 31 for different values of F_0^σ . The divergence at low temperature is due to the usual logarithmic correction (Altshuler, Aronov and Lee 1980; Finkelstein 1983, 1984; Castellani *et al* 1984).

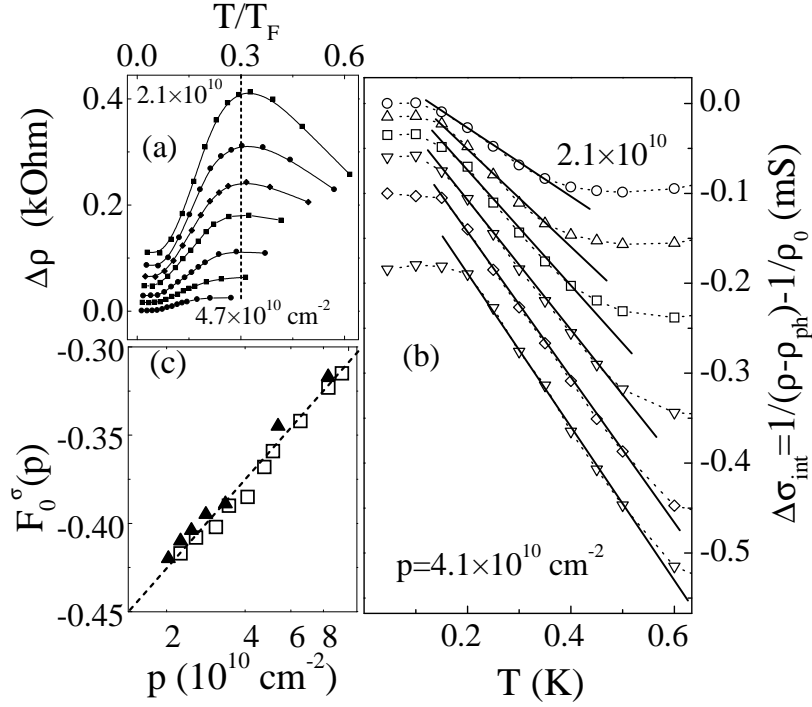


Figure 32. (a) $\Delta\rho$ as a function of the dimensionless temperature (T/T_F) at different p in a p -type GaAs/AlGaAs heterostructure. (For clarity, curves in (a) and (b) are offset vertically.) (b) The same data as in (a) plotted as conductivity, with linear fits. (c) Fermi liquid parameter versus hole density. Open symbols show the result obtained from the analysis of $\rho(T)$ at zero magnetic field; closed symbols show results obtained from the parallel-field magnetoresistance. From Proskuryakov *et al* (2002).

Although the exact value of F_0^σ cannot be calculated theoretically (in particular, its relation to the conventional measure of the interaction strength, r_s , is unknown for $r_s > 1$), it can in principle be found from a measurement of the Pauli spin susceptibility. The correction to the conductivity is almost always monotonic, except for a narrow region $-0.45 < F_0^\sigma < -0.25$.

As in the diffusive limit, magnetic field in the ballistic regime suppresses the correction in the triplet channel in Eq. (10), resulting in a universal, positive correction to the Drude conductivity in magnetic field, σ_0^B , and hence in the insulating-like behaviour of $\sigma(T)$:

$$\Delta\sigma = \sigma_0^B \frac{T}{T_F} \text{ at } B \geq B_s, \quad (11)$$

where B_s is the field corresponding to full spin polarization of the 2D system.

Proskuryakov *et al* (2002) were the first to perform a quantitative comparison of experimental data (obtained on p -type GaAs/AlGaAs) with the above theory. Their data for the temperature-induced corrections to the conductivity are plotted in Fig. 32 (b). (To extract corrections to the conductivity, Proskuryakov *et al* used

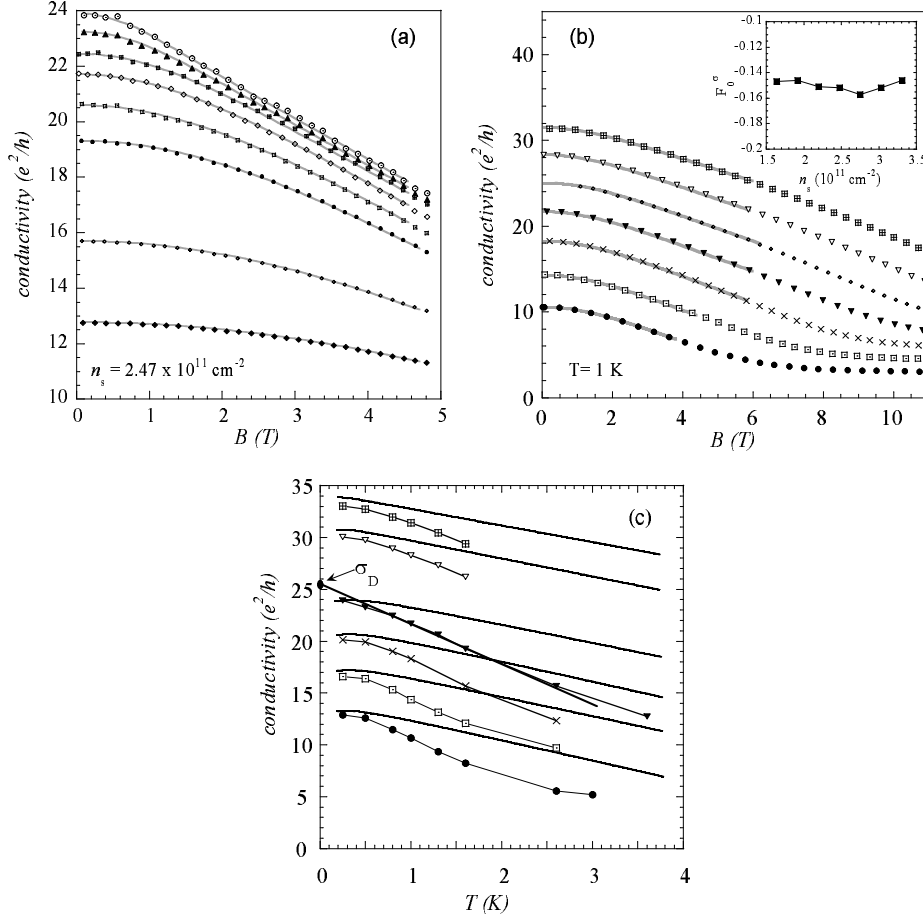


Figure 33. For parameters $\Delta = 1 \text{ K}$ and $F_0^\sigma = -0.15$, the magnetoconductivity of a silicon MOSFET: (a) For different temperatures at a fixed density $n_s = 2.47 \cdot 10^{11} \text{ cm}^{-2}$; $T = 0.25, 0.5, 0.8, 1.0, 1.3, 1.6, 2.6$ and 3.6 K (from top). (b) For different densities at a fixed temperature of 1 K ; $n_s = 3.3, 3.0, 2.75, 2.47, 2.19, 1.92$ and $1.64 \cdot 10^{11} \text{ cm}^{-2}$ (from top). (c) The conductivity as a function of temperature for the densities $n_s = 3.3, 3.0, 2.47, 2.19, 1.92$ and $1.64 \cdot 10^{11} \text{ cm}^{-2}$ (from top). Symbols and solid lines denote data and theory, respectively. From Vitkalov *et al* (2003).

the $\Delta\rho(T)$ dependence shown in Fig. 32 (a) obtained from raw resistivity data by subtracting the contribution of phonon scattering.) A linear fit of $\Delta\sigma(T)$ yields the parameter F_0^σ shown in Fig. 32 (c) for different p . The interaction constant obtained is negative and provides the metallic slope of $\sigma(T)$. As expected, the slope increases with decreasing density. When extrapolated to the crossover point from metallic to insulating behaviour ($p \approx 1.5 \cdot 10^{10} \text{ cm}^{-2}$), the interaction constant is much higher than the value of $F_0^\sigma = -1$ for the Stoner instability. The transition from metallic-like to insulating-like $\sigma(T)$ in their sample is unlikely to be related to any dramatic change in magnetic properties and is probably caused by Anderson localization.

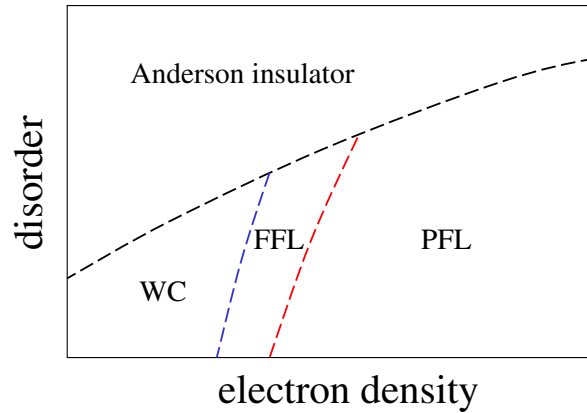


Figure 34. Schematic phase diagram corresponding to the numerical results of Attacalite *et al* 2002. The symbols WC, FFL and PFL correspond to the Wigner crystal, ferromagnetic Fermi liquid and paramagnetic Fermi liquid phases, respectively.

Comparison between the experimentally measured $\sigma(T)$ in the ballistic regime with the predictions of Zala *et al* was also carried out in silicon MOSFETs by Shashkin *et al* (2002; see sec. 4.2), Vitkalov *et al* (2003) and Pudalov *et al* (2003) (see also Das Sarma and Hwang 2003 and Shashkin *et al* 2003c) and in *p*-type SiGe heterostructures by Coleridge *et al* (2002). As shown in Fig. 33 (a) and (b), Vitkalov *et al* reported quantitative agreement between the theory and their magnetoresistance data in silicon MOSFETs. However, the values of the valley splitting Δ and Fermi liquid parameter F_0^σ required to obtain fits to the field dependence yield curves that are inconsistent with the observed temperature dependence in zero field, as shown in Fig. 33 (c). This was attributed to the neglect of additional scattering terms that affect the temperature dependence more strongly than the field dependence. Despite this quantitative discrepancy, the theory of Zala *et al* provides a reasonable description of the conductivity of strongly interacting 2D systems in the ballistic regime.

5.3. Approaches not based on Fermi liquid

The calculations of Finkelstein (1983, 1984), Castellani *et al* (1984) and Zala *et al* (2001) use the Fermi liquid as a starting point. As discussed earlier, r_s becomes so large that the theory's applicability is in question near the transition (Chamon *et al* 2001; for a review, see Varma *et al* 2002). Moreover, the behaviour of the effective mass reported by Shashkin *et al* (2003a, 2003b) in the vicinity of the transition is unlikely to be consistent with a Fermi liquid model.

Very little theory has been developed for strongly interacting systems for which r_s is large but below the expected Wigner crystallization. Several candidates have been suggested for the ground state of the strongly interacting 2D system, among them (i) a Wigner crystal characterized by spatial and spin ordering (Wigner 1934), (ii) an itinerant ferromagnet with spontaneous spin ordering (Stoner 1946), and (iii) a paramagnetic Fermi liquid (Landau 1957). According to numerical simulations (Tanatar and Ceperley 1989), Wigner crystallization is expected in a very dilute

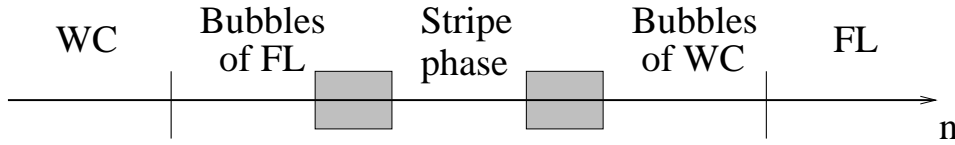


Figure 35. Phase diagram of the 2D electron system at $T = 0$ suggested by Spivak (2002). The symbols WC and FL correspond to the Wigner crystal and the Fermi liquid phases, respectively. The shaded regions correspond to phases which are more complicated than the bubble and the stripe phases.

regime, when r_s reaches approximately 35. This value has already been exceeded in the best p -type GaAs/AlGaAs heterostructures; however, no dramatic change in transport properties has occurred at the corresponding density. Recent detailed numerical simulations (Attacalite *et al* 2002) have predicted that in the range of the interaction parameter $25 < r_s < 35$ prior to the crystallization, the ground state of the system becomes an itinerant ferromagnet. The corresponding schematic phase diagram is shown in Fig. 34. As discussed earlier, there are experimental indications that a spontaneous spin polarization may occur at a finite electron density in silicon MOSFETs (and possibly in GaAs/AlGaAs heterostructures). Chakravarty *et al* (1999) have proposed a more complicated phase diagram where the low-density insulating state is a Wigner glass, a phase that has quasi-long-range translational order and competing ferromagnetic and antiferromagnetic spin-exchange interactions. The transition between insulating and metallic states within this theory is the melting of the Wigner glass, where the transition is second order due to the disorder.

Spivak (2002) predicted the existence of an intermediate phase between the Fermi liquid and the Wigner crystal with a first order transition in a clean electron system. The suggested phase diagram is shown in Fig. 35. In analogy with He^3 , where m^* increases approaching the crystallization point, Spivak (2001) suggested in an earlier paper that the renormalization of m^* is dominant compared to that of the g -factor as the transition is approached, and that m^* should increase with magnetic field. Although the increase of the mass is in agreement with the experimental results of Shashkin *et al* (2002, 2003a, 2003b), the suggested increase of m^* with the degree of spin polarization is not confirmed by their data. The strong increase of the effective mass near crystallization also follows from the approach used by Dolgoplov (2002), who has applied Gutzwiller's variational method (Brinkman and Rice 1970) to silicon MOSFETs, and from the dynamical mean-field theory (Tanasković *et al* 2003). However, the predicted dependence of m^* on the degree of spin polarization is again at odds with the experiment. Dharma-wardana (2003) has argued that in two-valley systems, correlation effects outweigh exchange, and a coupled-valley state is formed at $r_s \approx 5.4$ leading to strong enhancement of the effective mass, which in this case is only weakly dependent on the degree of spin polarization.

6. CONCLUSIONS

Significant progress has been achieved during the past few years in understanding the metallic state found a decade ago in strongly interacting 2D systems. There is now considerable evidence that the strong metallic temperature dependence of the resistance in these systems is due to the delocalizing effects of strong electron-

electron interactions. In ultra-clean silicon systems, the temperature dependence of the resistivity is universal near the metal-insulator transition and is quantitatively well described by the renormalization group theory; deep in the metallic state, in the ballistic regime, the temperature dependence of the resistance can be explained by coherent scattering of electrons by Friedel oscillations. In both cases, an external magnetic field quenches the delocalizing effect of interactions by aligning the spins, causing a giant positive magnetoresistance.

The metal-insulator transition is not yet understood theoretically. In silicon MOSFETs, various experimental methods provide evidence for a sharp increase and possible divergence of the spin susceptibility at some finite sample-independent electron density, n_χ , which is at or very near the critical density for the MIT in high mobility samples. Unlike the Stoner instability which entails an increase in the g -factor, the increase in the susceptibility in these systems is due to an increase of the effective mass. The effective mass is, in turn, found to be independent of the degree of spin polarization, implying that the increase is not due to spin exchange, in disagreement with the Fermi liquid model. A similar increase of the spin susceptibility is observed in GaAs/AlGaAs heterostructures, but it is not yet clear whether or not it points to a spontaneous spin polarization at a finite carrier density.

The fact that the $B = 0$ metal-insulator transition in the least disordered silicon samples occurs at or very close to n_χ indicates that the transition in such samples is a property of a clean electron system and is not driven by disorder. Quantum localization appears to be suppressed near the transition in these systems. In lower mobility samples, the localization transition occurs at electron densities much higher than n_χ and may be driven by disorder.

In closing, we note that most of the work done in these dilute two-dimensional systems concerns the transport behaviour, as transport measurements are relatively straightforward (despite problems associated with high impedance electrical contacts at low densities, the need to ensure proper cooling of the electrons system and so on). Studies done to date, many of which are reviewed here, include measurements of the resistivity as a function of temperature and magnetic field, the Hall coefficient, Shubnikov-de Haas oscillations and measurements of noise. Results have also been reported for the compressibility (Dultz and Jiang 2000; Ilani *et al* 2000, 2001; see also Si and Varma 1998 and Fogler 2003) and capacitive measurements (Khrapai *et al* 2003) from which one can obtain information about the chemical potential, the density of states, and which provide a measure of the magnetization, as discussed in sec. 4.1.

Many properties that would yield crucial information have not been investigated. Thermodynamic measurements such as specific heat and direct measurements of magnetization would be particularly illuminating; however, these are very difficult, if not impossible, to perform at this time due to the very small number of electrons available in a dilute, two-dimensional layer. Other experiments which could provide valuable information include tunnelling and different resonance techniques. Measurements of one, several, or perhaps all of these may be required for a full understanding of the enigmatic and very interesting behaviour of strongly interacting electrons (or holes) in two dimensions.

Acknowledgments

We are grateful to G B Bachelet, V T Dolgoplov, A M Finkelstein, T M Klapwijk, S Moroni, B N Narozhny, D Neilson, A A Shashkin, C Senatore, B Spivak and S A Vitkalov for useful discussions. SVK is supported by the National Science Foundation grant DMR-0129652 and the Sloan Foundation; MPS is supported by Department of Energy grant no. DE-FG02-84ER45153 and National Science Foundation grant DMR-0129581.

7. REFERENCES

- Abrahams E, Anderson P W, Licciardello D C and Ramakrishnan T V 1979 Scaling theory of localization: Absence of quantum diffusion in two dimensions *Phys. Rev. Lett.* **42** 673-676
- Abrahams E, Kravchenko S V and Sarachik M P 2001 Metallic behavior and related phenomena in two dimensions *Rev. Mod. Phys.* **73** 251-266
- Altshuler B L, Aronov A G and Lee P A 1980 Interaction effects in disordered Fermi systems in two dimensions *Phys. Rev. Lett.* **44** 1288-1291
- Altshuler B L and Maslov D L 1999 Theory of metal-insulator transitions in gated semiconductors *Phys. Rev. Lett.* **82** 145-148
- Altshuler B L, Maslov D L and Pudalov V M 2000 Metal-insulator transition in 2D: Anderson localization in temperature-dependent disorder? *Phys. Status Solidi b* **218** 193-200
- Altshuler B L, Maslov D L and Pudalov V M 2001 Metal-insulator transition in 2D: resistance in the critical region *Physica E* **9** 209-225
- Ando T, Fowler A B and Stern F 1982 Electronic-properties of two-dimensional systems *Rev. Mod. Phys.* **54** 437-672
- Attacalite C, Moroni S, Gori-Giorgi P and Bachelet G B 2002 Correlation energy and spin polarization in the 2D electron gas *Phys. Rev. Lett.* **88** 256601
- Batke E and Tu C W 1986 Effective mass of a space-charge layer on GaAs in a parallel magnetic-field *Phys. Rev. B* **34** 3027-3029
- Bishop D J, Tsui D C and Dynes R C 1980 Nonmetallic conduction in electron inversion layers at low temperatures *Phys. Rev. Lett.* **44** 1153-1156
- Bishop D J, Dynes R C and Tsui D C 1982 Magnetoresistance in Si metal-oxide-semiconductor field-effect transistors – evidence of weak localization and correlation *Phys. Rev. B* **26** 773-779
- Bogdanovich S and Popović D 2002 Onset of glassy dynamics in a two-dimensional electron system in silicon *Phys. Rev. Lett.* **88** 236401
- Brinkman W F and Rice T M 1970 Application of Gutzwiller's variational method to the metal-insulator transition *Phys. Rev. B* **2** 4302-4304
- Brunthaler G, Prinz A, Bauer G and Pudalov V M 2001 Exclusion of quantum coherence as the origin of the 2D metallic state in high-mobility silicon inversion layers *Phys. Rev. Lett.* **87** 096802
- Castellani C, Di Castro C, Lee P A and Ma M 1984 Interaction-driven metal-insulator transitions in disordered fermion systems *Phys. Rev. B* **30** 527-543
- Castellani C, Di Castro C and Lee P A 1998 Metallic phase and metal-insulator transition in two-dimensional electronic systems *Phys. Rev. B* **57** R9381-R9384
- Chakravarty S, Kivelson S, Nayak C and Voelker K 1999 Wigner glass, spin liquids and the metal-insulator transition *Phil. Mag. B* **79** 859-868
- Chamon C, Mucciolo E R and Castro Neto A H 2001 *P*-wave pairing and ferromagnetism in the metal-insulator transition in two dimensions *Phys. Rev. B* **64** 245115
- Chen G-H and Raikh M E 1999 Exchange-induced enhancement of spin-orbit coupling in two-dimensional electronic systems *Phys. Rev. B* **60** 4826-4833
- Coleridge P T, Williams R L, Feng Y and Zawadzki P 1997 Metal-insulator transition at $B = 0$ in *p*-type SiGe *Phys. Rev. B* **56** R12764-R12767
- Coleridge P T, Sachrajda AS and Zawadzki P 2002 Weak localization, interaction effects, and the metallic phase in *p*-SiGe *Phys. Rev. B* **65** 125328
- Das Sarma S 1986 Theory of finite-temperature screening in a disordered two-dimensional electron-gas *Phys. Rev. B* **33** 5401-5405
- Das Sarma S and Hwang E H 1999 Charged impurity-scattering-limited low-temperature resistivity of low-density silicon inversion layers *Phys. Rev. Lett.* **83** 164-167
- Das Sarma S and Hwang E H 2000 Parallel magnetic field induced giant magnetoresistance in low density quasi-two-dimensional layers *Phys. Rev. Lett.* **84** 5596-5599

- Das Sarma S and Hwang E H 2003 On the temperature dependence of 2D “metallic” conductivity in Si inversion layers at intermediate temperatures *Preprint cond-mat/0310260*
- Dharma-wardana M W C 2003 The effective mass and the g-factor of the strongly-correlated 2-D electron fluid: Evidence of a coupled-valley state in the Si system *Preprint cond-mat/0307153*
- Dobrosavljević V, Abrahams E, Miranda E and Chakravarty S 1997 Scaling theory of two-dimensional metal-insulator transitions *Phys. Rev. Lett.* **79** 455-458
- Dolan G J and Osheroff D D 1979 Nonmetallic conduction in thin metal films at low temperatures *Phys. Rev. Lett.* **43** 721-724
- Dolgoplov V T, Kravchenko G V, Shashkin A A and Kravchenko S V 1992 Properties of electron insulating phase in Si inversion-layers at low-temperatures *JETP Lett.* **55** 733-737
- Dolgoplov V T and Gold A 2000 Magnetoresistance of a two-dimensional electron gas in a parallel magnetic field *JETP Lett.* **71** 27-30
- Dolgoplov V T 2002 On effective electron mass of silicon field structures at low electron densities *JETP Lett.* **76** 377-379
- Dolgoplov V T and Gold A 2002 Comment on “Weak anisotropy and disorder dependence of the in-plane magnetoresistance in high-mobility (100) Si-inversion layers” *Phys. Rev. Lett.* **89** 129701
- Dultz S C and Jiang H W 2000 Thermodynamic signature of a two-dimensional metal-insulator transition *Phys. Rev. Lett.* **84** 4689-4692
- Efros A L and Shklovskii B I 1975 Coulomb gap and low temperature conductivity of disordered systems *J. Phys. C: Solid State Phys.* **8** L49-L51
- Fang F F and Stiles P J 1968 Effects of a tilted magnetic field on a two-dimensional electron gas *Phys. Rev.* **174** 823-828
- Finkelstein A M 1983 Influence of Coulomb interaction on the properties of disordered metals *Sov. Phys. — JETP* **57** 97-108
- Finkelstein A M 1984 Weak localization and coulomb interaction in disordered-systems *Z. Phys. B* **56** 189-196
- Fogler M M 2003 Nonlinear screening and percolative transition in a two-dimensional electron liquid *Preprint cond-mat/0310010*
- Gao X P A, Mills A P, Ramirez A P, Pfeiffer L N and West K W 2002 Weak-localization-like temperature-dependent conductivity of a dilute two-dimensional hole gas in a parallel magnetic field *Phys. Rev. Lett.* **89** 016801
- Gold A and Dolgoplov V T 1986 Temperature dependence of the conductivity for the two-dimensional electron gas: Analytical results for low temperatures *Phys. Rev. B* **33** 1076-1084
- Gold A 2001 Linear temperature dependence of mobility in quantum wells and the effects of exchange and correlation *J. Phys.: Condens. Matter* **13** 11641-11650
- Gold A and Dolgoplov V T 2002 On the role of disorder in transport and magnetic properties of the two-dimensional electron gas *J. Phys.: Condens. Matter* **14** 7091-7096
- Gold A 2003 Linear temperature dependence of the mobility in two-dimensional electron gases: many-body and spin-polarization effects *J. Phys.: Condens. Matter* **15** 217-223
- Hanein Y, Meirav U, Shahar D, Li C C, Tsui D C and Shtrikman H 1998a The metalliclike conductivity of a two-dimensional hole system *Phys. Rev. Lett.* **80** 1288-1291
- Hanein Y, Shahar D, Yoon J, Li C C, Tsui D C and Shtrikman H 1998b Properties of the apparent metal-insulator transition in two-dimensional systems *Phys. Rev. B* **58** R7520-R7523
- Heemskerk R and Klapwijk T M 1998 Nonlinear resistivity at the metal-insulator transition in a two-dimensional electron gas *Phys. Rev. B* **58** R1754-R1757
- Herbut I F 2001 The effect of a parallel magnetic field on the Boltzmann conductivity and the Hall coefficient of a disordered two dimensional Fermi liquid *Phys. Rev. B* **63** 113102
- Hikami S, Larkin A I and Nagaoka Y 1980 Spin-orbit interaction and magnetoresistance in the two dimensional random system *Prog. Theor. Phys.* **63** 707-710
- Ilani S, Yacoby A, Mahalu D and Shtrikman H 2000 Unexpected behavior of the local compressibility near the $B = 0$ metal-insulator transition *Phys. Rev. Lett.* **84** 3133-3136
- Ilani S, Yacoby A, Mahalu D and Shtrikman H 2001 Microscopic structure of the metal-insulator transition in two dimensions *Science* **292** 1354-1357
- Iwamoto N 1991 Static local-field corrections of 2-dimensional electron liquids *Phys. Rev. B* **43** 2174-2182
- Jaroszyński J, Popović D and Klapwijk T M 2002 Universal behavior of the resistance noise across the metal-insulator transition in silicon inversion layers *Phys. Rev. Lett.* **89** 276401
- Khrapai V S, Shashkin A A and Dolgoplov V T 2003 Direct measurements of the spin and the cyclotron gaps in a 2D electron system in silicon *Phys. Rev. Lett.* **91** 126404
- Kravchenko S V, Kravchenko G V, Furneaux J E, Pudalov V M and D'Iorio M 1994 Possible metal-insulator-transition at $B = 0$ in 2 dimensions *Phys. Rev. B* **50** 8039-8042

- Kravchenko S V, Mason W E, Bowker G E, Furneaux J E, Pudalov V M and D'Iorio M 1995 Scaling of an anomalous metal-insulator-transition in a 2-dimensional system in silicon at $B = 0$ *Phys. Rev. B* **51** 7038-7045
- Kravchenko S V, Simonian D, Sarachik M P, Mason W and Furneaux J E 1996 Electric field scaling at a $B = 0$ metal-insulator transition in two dimensions *Phys. Rev. Lett.* **77** 4938-4941
- Kravchenko S V, Simonian D, Sarachik M P, Kent A D and Pudalov V M 1998 Effect of a tilted magnetic field on the anomalous $H = 0$ conducting phase in high-mobility Si MOSFET's *Phys. Rev. B* **58** 3553-3556
- Kravchenko S V and Klapwijk T M 2000a Metallic low-temperature resistivity in a 2D electron system over an extended temperature range *Phys. Rev. Lett.* **84** 2909-2912
- Kravchenko S V, Shashkin A A, Bloore D A and Klapwijk T M 2000b Shubnikov-de Haas oscillations near the metal-insulator transition in a two-dimensional electron system in silicon *Solid State Commun.* **116** 495-499
- Kravchenko S V, Shashkin A A and Dolgoplov V T 2002 Comment on "Low-density spin susceptibility and effective mass of mobile electrons in Si inversion layers" *Phys. Rev. Lett.* **89** 219701
- Kwon Y, Ceperley D M and Martin R M 1994 Quantum Monte-Carlo calculation of the Fermi-liquid parameters in the 2-dimensional electron-gas *Phys. Rev. B* **50** 1684-1694
- Landau L D 1957 The theory of a Fermi liquid *Sov. Phys. — JETP* **3** 920-925
- Lee P A and Ramakrishnan T V 1982 Magnetoresistance of weakly disordered electrons *Phys. Rev. B* **26** 4009-4012
- Lee P A and Ramakrishnan T V 1985 Disordered electronic systems *Rev. Mod. Phys.* **57** 287-337
- Lilly M P, Reno J L, Simmons J A, Spielman I B, Eisenstein J P, Pfeiffer L N, West K W, Hwang E H and Das Sarma S 2003 Resistivity of dilute 2D electrons in an undoped GaAs heterostructure *Phys. Rev. Lett.* **90** 056806
- Mason W, Kravchenko S V, Bowker G E and Furneaux J E 1995 Experimental evidence for a Coulomb gap in 2 dimensions *Phys. Rev. B* **52** 7857-7859
- Mertes K M, Zheng H, Vitkalov S A, Sarachik P and Klapwijk T M 2001 Temperature dependence of the resistivity of a dilute two-dimensional electron system in high parallel magnetic field *Phys. Rev. B* **63** 041101(R)
- Mills A P, Ramirez A P, Pfeiffer L N and West K W 1999 Nonmonotonic temperature-dependent resistance in low density 2D hole gases *Phys. Rev. Lett.* **83** 2805-2808
- Mills A P, Ramirez A P, Gao X P A, Pfeiffer L N, West K W and Simon S H 2001 Suppression of weak localization effects in low-density metallic 2D holes *Preprint cond-mat/0101020*
- Noh H, Lilly M P, Tsui D C, Simmons J A, Hwang E H, Das Sarma S, Pfeiffer L N and West K W 2002 Interaction corrections to two-dimensional hole transport in the large r_s limit *Phys. Rev. B* **68** 165308
- Okamoto T, Hosoya K, Kawaji S and Yagi A 1999 Spin degree of freedom in a two-dimensional electron liquid *Phys. Rev. Lett.* **82** 3875-3878
- Papadakis S J and Shayegan M 1998 Apparent metallic behavior at $B = 0$ of a two-dimensional electron system in AlAs *Phys. Rev. B* **57** R15068-R15071
- Papadakis S J, De Poortere E P, Shayegan M and Winkler R 2000 Anisotropic magnetoresistance of two-dimensional holes in GaAs *Phys. Rev. Lett.* **84** 5592-5595
- Pastor A A and Dobrosavljević V 1999 Melting of the electron glass *Phys. Rev. Lett.* **83** 4642-4645
- Pepper M, Pollitt S and Adkins C J 1974 The spatial extent of localized state wavefunctions in silicon inversion layers *J. Phys. C: Solid State Phys.* **7** L273-L277
- Phillips P, Wan Y, Martin I, Knysh S and Dalidovich D 1998 Superconductivity in a two-dimensional electron gas *Nature (London)* **395** 253-257
- Polyakov D G and Shklovskii B I 1993 Conductivity-peak broadening in the quantum Hall regime *Phys. Rev. B* **48** 11167-11175
- Popović D, Fowler A B and Washburn S 1997 Metal-insulator transition in two dimensions: Effects of disorder and magnetic field *Phys. Rev. Lett.* **79** 1543-1546
- Proskuryakov Y Y, Savchenko A K, Safonov S S, Pepper M, Simmons M Y and Ritchie D A 2002 Hole-hole interaction effect in the conductance of the two-dimensional hole gas in the ballistic regime *Phys. Rev. Lett.* **89** 076406
- Prus O, Reznikov M, Sivan U and Pudalov V M 2002 Cooling of electrons in a silicon inversion layer *Phys. Rev. Lett.* **88** 016801
- Prus O, Yaish Y, Reznikov M, Sivan U and Pudalov V M 2003 Thermodynamic spin magnetization of strongly correlated two-dimensional electrons in a silicon inversion layer *Phys. Rev. B* **67** 205407
- Pudalov V M, D'Iorio M, Kravchenko S V and Campbell J W 1993 Zero magnetic field collective insulator phase in a dilute 2D electron system *Phys. Rev. Lett.* **70** 1866-1869

- Pudalov V M, Brunthaler G, Prinz A and Bauer G 1997 Instability of the two-dimensional metallic phase to a parallel magnetic field *JETP Lett.* **65** 932-937
- Pudalov V M, Brunthaler G, Prinz A and Bauer G 1998 Metal-insulator transition in two dimensions *Physica E* **3** 79-88
- Pudalov V M, Brunthaler G, Prinz A and Bauer G 1999 Weak-field Hall resistance and effective carrier density measurements across the metal-insulator transition in Si-MOS structures *JETP Lett.* **70** 48-53
- Pudalov V M, Brunthaler G, Prinz A and Bauer G 2001 Effect of the in-plane magnetic field on conduction of the Si-inversion layer: magnetic field driven disorder *Preprint cond-mat/0103087*
- Pudalov V M, Brunthaler G, Prinz A and Bauer G 2002a Weak anisotropy and disorder dependence of the in-plane magnetoresistance in high-mobility (100) Si-inversion layers *Phys. Rev. Lett.* **88** 076401
- Pudalov V M, Gershenson M E, Kojima H, Butch N, Dizhur E M, Brunthaler G, Prinz A and Bauer G 2002b Low-density spin susceptibility and effective mass of mobile electrons in Si inversion layers *Phys. Rev. Lett.* **88** 196404
- Pudalov V M, Gershenson M E, Kojima H, Brunthaler G, Prinz A and Bauer G 2003 Interaction effects in conductivity of Si inversion layers at intermediate temperatures *Phys. Rev. Lett.* **91** 126403
- Punnoose A and Finkelstein A M 2002 Dilute electron gas near the metal-insulator transition: Role of valleys in silicon inversion layers *Phys. Rev. Lett.* **88** 016802
- Rahimi M, Anissimova S, Sakr M R, Kravchenko S V and Klapwijk T M 2003 Coherent back-scattering near the two-dimensional metal-insulator transition *Phys. Rev. Lett.* **91** 116402
- Sarachik M P and Kravchenko S V 1999 Novel phenomena in dilute electron systems in two dimensions *Proc. Natl. Acad. Sci. USA* **96** 5900-5902
- Sarachik M P 2002 Disorder-dependence of the critical density in two-dimensional systems: An empirical relation *Europhys. Lett.* **57** 546-549
- Sarachik M P and Vitkalov S A 2003 Does m^*g^* diverge at a finite electron density in silicon inversion layers? *J. Phys. Soc. Japan (Suppl. A)* **72** 57-62
- Senz V, Dötsch U, Gennser U, Ihn T, Heinzel T, Ensslin K, Hartmann R and Grützmacher D 1999 Metal-insulator transition in a 2-dimensional system with an easy spin axis *Ann. Phys., Lpz.* **8** (special issue) 237-240
- Shahar D, Tsui D C, Shayegan M, Cunningham J E, Shimshoni E and Sondhi S L 1996 Evidence for charge-flux duality near the quantum Hall liquid-to-insulator transition *Science* **274** 589-592
- Shashkin A A, Dolgoplov V T and Kravchenko G V 1994 Insulating phases in a 2-dimensional electron-system of high-mobility Si MOSFETs *Phys. Rev. B* **49** 14486-14495
- Shashkin A A, Kravchenko S V, Dolgoplov V T and Klapwijk T M 2001a Indication of the ferromagnetic instability in a dilute two-dimensional electron system *Phys. Rev. Lett.* **87**, 086801
- Shashkin A A, Kravchenko S V and Klapwijk T M 2001b Metal-insulator transition in 2D: equivalence of two approaches for determining the critical point *Phys. Rev. Lett.* **87**, 266402
- Shashkin A A, Kravchenko S V, Dolgoplov V T and Klapwijk T M 2002 Sharp increase of the effective mass near the critical density in a metallic two-dimensional electron system *Phys. Rev. B* **66** 073303
- Shashkin A A, Rahimi M, Anissimova S, Kravchenko S V, Dolgoplov V T and Klapwijk T M 2003a Spin-independent origin of the strongly enhanced effective mass in a dilute 2D electron system *Phys. Rev. Lett.* **91** 046403
- Shashkin A A, Kravchenko S V, Dolgoplov V T and Klapwijk T M 2003b Sharply increasing effective mass: a precursor of a spontaneous spin polarization in a dilute two-dimensional electron system *J. Phys. A: Math. Gen.* **36** 9237-9247
- Shashkin A A, Dolgoplov V T and Kravchenko S V 2003c Comment on "Interaction effects in conductivity of Si inversion layers at intermediate temperatures" *Preprint cond-mat/0311174*
- Si Q M and Varma C M 1998 Metal-insulator transition of disordered interacting electrons *Phys. Rev. Lett.* **81** 4951-4954
- Simmons M Y, Hamilton A R, Pepper M, Linfield E H, Rose P D, Ritchie D A, Savchenko A K and Griffiths T G 1998 Metal-insulator transition at $B = 0$ in a dilute two dimensional GaAs-AlGaAs hole gas *Phys. Rev. Lett.* **80** 1292-1295
- Simmons M Y, Hamilton A R, Pepper M, Linfield E H, Rose P D and Ritchie D A 2000 Weak localization, hole-hole interactions, and the "metal"-insulator transition in two dimensions *Phys. Rev. Lett.* **84** 2489-2492
- Simonian D, Kravchenko S V and Sarachik M P 1997a Reflection symmetry at a $B = 0$ metal-insulator transition in two dimensions *Phys. Rev. B* **55** R13421-R13423
- Simonian D, Kravchenko S V, Sarachik M P and Pudalov V M 1997b Magnetic field suppression of

- the conducting phase in two dimensions *Phys. Rev. Lett.* **79** 2304-2307
- Simonian D, Kravchenko S V, Sarachik M P and Pudalov V M 1998 H/T scaling of the magnetoconductance near the conductor-insulator transition in two dimensions *Phys. Rev. B* **57** R9420-R9422
- Smith J L and Stiles P J 1972 Electron-electron interactions continuously variable in the range $2.1 > r_s > 0.9$ *Phys. Rev. Lett.* **29** 102-104
- Sondhi S L, Girvin S M, Carini J P and Shahar D 1997 Continuous quantum phase transitions *Rev. Mod. Phys.* **69** 315-333
- Spivak B 2001 Properties of the strongly correlated two-dimensional electron gas in Si MOSFET's *Phys. Rev. B* **64** 085317
- Spivak B 2002 Phase separation in the two-dimensional electron liquid in MOSFET's *Phys. Rev. B* **67** 125205
- Stern F 1980 Calculated temperature dependence of mobility in silicon inversion layers *Phys. Rev. Lett.* **44** 1469-1472
- Stoner E C 1946 Ferromagnetism *Rep. Prog. Phys.* **11** 43-112
- Tanasković D, Dobrosavljević V, Abrahams E and Kotliar G 2003 Disorder screening in strongly correlated systems *Phys. Rev. Lett.* **91** 066603
- Tanatar B and Ceperley D M 1989 Ground-state of the two-dimensional electron-gas *Phys. Rev. B* **39** 5005-5016
- Tutuc E, De Poortere E P, Papadakis S J and Shayegan M 2001 In-plane magnetic field-induced spin polarization and transition to insulating behavior in two-dimensional hole systems *Phys. Rev. Lett.* **86** 2858-2861
- Tutuc E, Melinte S and Shayegan M 2002 Spin polarization and g factor of a dilute GaAs two-dimensional electron system *Phys. Rev. Lett.* **88** 36805
- Tutuc E, Melinte S, De Poortere E P, Shayegan M and Winkler R 2003 Role of finite layer thickness in spin polarization of GaAs two-dimensional electrons in strong parallel magnetic fields *Phys. Rev. B* **67** 241309(R)
- Uren M J, Davies R A and Pepper M 1980 The observation of interaction and localisation effects in a two-dimensional electron gas at low temperatures *J. Phys. C: Solid State Phys.* **13** L985-L993
- Varma C M, Nussinov Z and van Saarloos W 2002 Singular or non-Fermi liquids *Phys. Rep.* **361** 267-417
- Vitkalov S A, Zheng H, Mertes K M, Sarachik M P and Klapwijk Y M 2000 Small-angle Shubnikov-de Haas measurements in a 2D electron system: The effect of a strong in-plane magnetic field *Phys. Rev. Lett.* **85** 2164-2167
- Vitkalov S A, Sarachik M P and Klapwijk T M 2001a Spin polarization of two-dimensional electrons determined from Shubnikov-de Haas oscillations as a function of angle *Phys. Rev. B* **64** 073101
- Vitkalov S A, Zheng H, Mertes K M, Sarachik M P and Klapwijk T M 2001b Scaling of the magnetoconductivity of silicon MOSFETs: Evidence for a quantum phase transition in two dimensions *Phys. Rev. Lett.* **87** 086401
- Vitkalov S A, Sarachik M P and Klapwijk T M 2002 Spin polarization of strongly interacting two-dimensional electrons: The role of disorder *Phys. Rev. B* **65** 201106(R)
- Vitkalov S A, James K, Narozhny B N, Sarachik M P and Klapwijk T M 2003 In-plane magnetoconductivity of Si MOSFETs: A quantitative comparison of theory and experiment *Phys. Rev. B* **67** 113310
- Vojta M 2003 Quantum phase transitions *Rep. Prog. Phys.* **66** 2069-2110
- Wigner E 1934 On the interaction of electrons in metals *Phys. Rev.* **46** 1002-1011
- Yaish Y, Prus O, Buchstab E, Shapira S, Ben Yoseph G, Sivan U and Stern A 2000 Interband scattering and the "metallic phase" of two-dimensional holes in GaAs/AlGaAs *Phys. Rev. Lett.* **84** 4954-4957
- Yoon J, Li C C, Shahar D, Tsui D C and Shayegan M 1999 Wigner crystallization and metal-insulator transition of two-dimensional holes in GaAs at $B = 0$ *Phys. Rev. Lett.* **82** 1744-1747
- Yoon J, Li C C, Shahar D, Tsui D C and Shayegan M 2000 Parallel magnetic field induced transition in transport in the dilute two-dimensional hole system in GaAs *Phys. Rev. Lett.* **84** 4421-4424
- Zala G, Narozhny B N and Aleiner I L 2001 Interaction corrections at intermediate temperatures: Longitudinal conductivity and kinetic equation *Phys. Rev. B* **64** 214204
- Zala G, Narozhny B N and Aleiner I L 2002 Interaction corrections at intermediate temperatures: Magnetoresistance in a parallel field *Phys. Rev. B* **65** 020201(R)
- Zhu J, Stormer H L, Pfeiffer L N, Baldwin K W and West K W 2003 Spin susceptibility of an ultra-low-density two-dimensional electron system *Phys. Rev. Lett.* **90** 056805